Nano Research

ISSN 1998-0124 CN 11-5974/O4
https://doi.org/10.26599/NR.2026.94908530

Review Article

Flexible alternating current electroluminescence devices toward sensing-display integration

Kai Xue[2,3,§], Yuzhu Li[2,3,§], Pingping Cai[2,3,§], Zhitao Zhang[1,2,3,4](✉)

[1] Macao Translational Medicine Center, Macau University of Science and Technology, Taipa 999078, Macau, China

[2] State Key Laboratory of Synergistic Chem-Bio Synthesis, School of Chemistry and Chemical Engineering, Shanghai Jiao Tong University, Shanghai 200240, China

[3] Zhangjiang Institute for Advanced Study, Shanghai Jiao Tong University, Shanghai 200240, China

[4] The International Peace Maternity and Child Health Hospital, School of Medicine, Shanghai Jiao Tong University, National Center for Translational Medicine, Xi'an 200030, China

[§] Kai Xue, Yuzhu Li, and Pingping Cai contributed equally to this work.

Nano Res., **Just Accepted Manuscript** • https://doi.org/10.26599/NR.2026.94908530

https://www.sciopen.com/journal/1998-0124 on Feb. 3, 2026

Just Accepted

TABLE OF CONTENTS (TOC)

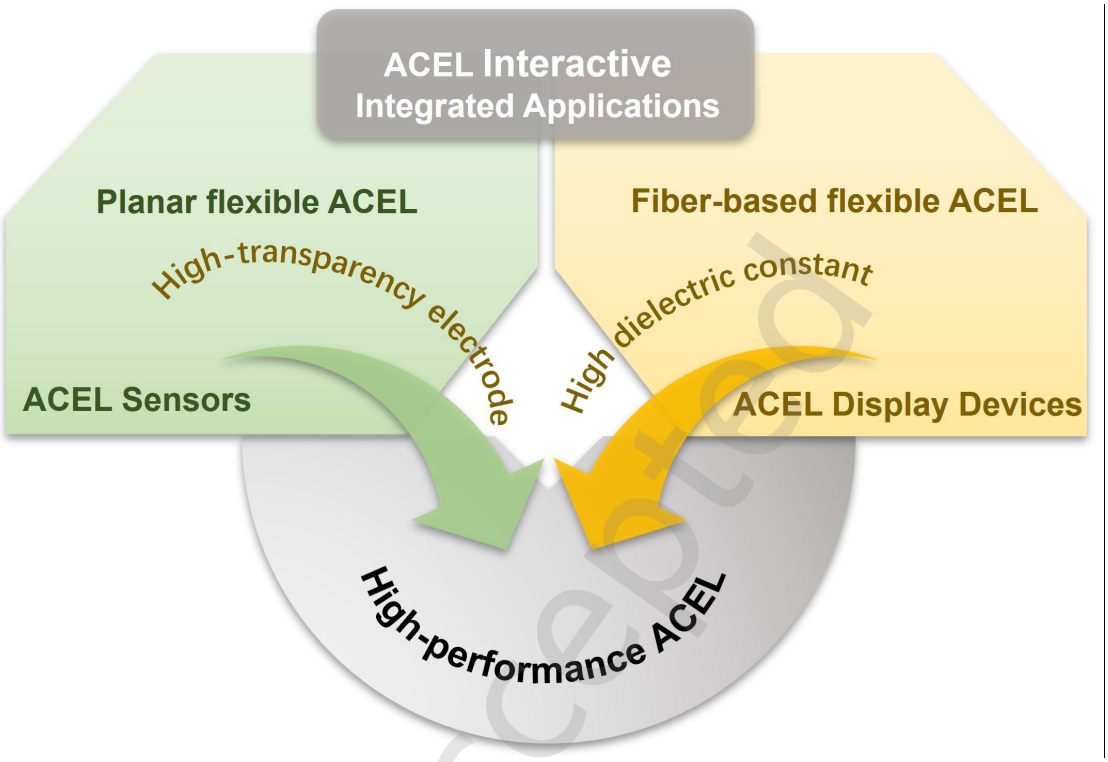

This review provides a comprehensive overview of flexible ACEL devices, focusing on planar and fiber structures and their applications in display and visual sensing.

Review Article

Flexible alternating current electroluminescence devices toward sensing-display integration

Kai Xue[2,3,§], *Yuzhu Li*[2,3,§], *Pingping Cai*[2,3,§], *and Zhitao Zhang*[1,2,3,4] ✉

[1]Macao Translational Medicine Center, Macau University of Science and Technology, Taipa 999078, Macau, China

[2]State Key Laboratory of Synergistic Chem-Bio Synthesis, School of Chemistry and Chemical Engineering, Shanghai Jiao Tong University, Shanghai 200240, China

[3]Zhangjiang Institute for Advanced Study, Shanghai Jiao Tong University, Shanghai 200240, China

[4]The International Peace Maternity and Child Health Hospital, School of Medicine, Shanghai Jiao Tong University, National Center for Translational Medicine, Xi'an 200030, China

[§]Kai Xue, Yuzhu Li, and Pingping Cai contributed equally to this work.

Received: 2 December 2025; **Revised:** 1 February 2026; **Accepted:** 3 February 2026

✉Address correspondence to zhangzhitao@sjtu.edu.cn

Cite this article: *Nano Research*, **2026**, *19*, 94908530. https://doi.org/10.26599/NR.2026.94908530

Abstract

The burgeoning advancement of flexible electronics necessitates the development of light-emitting devices that integrate high performance with multifunctional capabilities. Zinc sulfide alternating current electroluminescent (ACEL) devices, leveraging their inherent flexibility, exceptional environmental stability, and area light source characteristics, have emerged as one of the most promising platforms for constructing next-generation wearable optoelectronic devices. However, further advancement is constrained by multiple challenges, including driving voltage requirements, environmental stability, and scalable manufacturing. This review offers a critical synthesis of recent advances through a unique "materials–device–system" co-evolution lens, a perspective underexplored in prior literature. It systematically elucidates electroluminescence mechanisms and performance‐ tuning strategies for key components (emissive layers, dielectric layers, and electrodes), while simultaneously mapping the field's progression through three defining phases: static displays, dynamic pixelated displays, and intelligent interactive systems. Collectively, this review aims to serve as a valuable resource by providing critical insights to guide future development of high-performance flexible ACEL devices.

Keywords: alternating current electroluminescent devices, flexible displays, sensors, human-computer interaction interface

1. Introduction

Flexible electronics has garnered significant attention due to its advantages over conventional rigid devices, including conformability to irregular surfaces, mechanical robustness under deformation, and enhanced integration with physiological systems. Driven by the rapid advancements in artificial intelligence and this material paradigm shift, human-computer interaction is undergoing a fundamental transformation from rigid, planar interfaces toward flexible, conformable designs [1]. This evolution necessitates that future light-emitting displays not only deliver high brightness and superior color performance but also incorporate essential characteristics such as flexibility and stretchability. Such mechanical compliance is crucial for enabling intimate integration with the human body, thereby paving the way for novel applications in displays, lighting [2-4], sensing [5-9], and medical healthcare [10-12].

To realize this vision, alternating current electroluminescence (ACEL) technology, particularly zinc sulfide (ZnS)-based systems, has emerged as a promising solution [13-20]. As illustrated in **Fig. 1**, flexible ACEL devices enable unique functional integration and offer diverse application potential. When compared with conventional displays like liquid crystal displays (LCDs) [21] and organic light-emitting diodes (OLEDs) [22-25], ACEL devices exhibit inherent flexibility, robust mechanical durability, architectural simplicity, and strong resilience in complex environments [26-28]. These advantages position them as highly suitable candidates for wearable intelligent systems and visual sensing platforms. In recent years, through synergistic innovations in phosphor materials, dielectric components, and flexible electrodes/substrates, significant progress has been achieved in flexible ACEL devices, including substantial reductions in driving voltage (to within the human safety threshold), enhanced luminance, and the realization of multi-color and full-color emission [29-32].

Despite these promising developments, the widespread deployment of ACEL technology in future applications such as artificial intelligence, intelligent robotics, and human-machine interaction continues to face challenges related to driving voltage requirements, device brightness and long-term stability, material system optimization,

and multifunctional integration [33,34]. This review systematizes recent advances in flexible ACEL devices, covering their fundamental working mechanisms, performance modulation strategies for key components (luminescent layers, dielectric layers, and electrode structures), and emerging applications in cutting-edge fields such as stretchable displays and optical sensing. A forward-looking perspective is also offered to guide future research and inspire continued progress in this rapidly evolving domain.

2. Mechanisms and Preparation Process of ACEL Devices

2.1. Mechanisms

ACEL is a physical phenomenon in which electrical energy is directly converted into light energy under the excitation of a high-intensity alternating electric field. Among various ACEL devices, powder-based systems employing ZnS doped with metal activators such as copper (Cu), are especially promising for flexible displays and visual sensing. Their distinctive surface-emission characteristics, combined with a simple architecture and mechanical flexibility, make them highly attractive for these applications [47,48].

A conventional ACEL device functions analogously to a luminous parallel-plate capacitor. Its core structure comprises a luminescent layer of ZnS-based phosphor particles dispersed in a dielectric matrix sandwiched between two conductive electrodes. Upon application of an alternating electric field, luminescent centers within the phosphor particles are activated through carrier excitation, resulting in light emission (**Fig. 2(a)**) [50-53]. Device fabrication typically employs solution-processing techniques such as printing or coating, enabling cost-effective and large-area production.

Extensive research has established that light emission is closely associated with Cu_xS heterojunctions formed within the ZnS crystal lattice [54]. Under a high-voltage alternating electric field, electrons tunnel from the Cu_xS nanodomains into ZnS host matrix, where they are temporarily trapped at defect or impurity energy levels. During

the reverse half-cycle of the electric field, these trapped electrons are released and recombine radiatively with holes, resulting in photon emission (**Fig. 2(b)**) [40,55,56]. By modulating the host composition (e.g., Zn(S,Se)) or substituting different activator ions (such as Cu, Mn, Ag, etc.), broadband tunable emissions spanning from blue to red can be achieved, fulfilling diverse color requirements across various application domains.

Currently, flexible ACEL devices can be broadly categorized into two types: planar flexible ACEL devices and fiber-based flexible ACEL [57,58] devices, serving distinct application scenarios. A representative example of a planar configuration is illustrated in **Fig. 2(c)** [40]. In comparison, fiber-based ACEL devices employ polymer or conductive fibers as the structural substrate [59]. A typical fiber-shaped device architecture is depicted in **Fig. 2(d)** [40]. When an insulating polymer serves as the substrate, electrodes must be fabricated on its surface through a multi-step process, followed by the sequential deposition of the dielectric layer and the luminescent layer [60]. The outermost electrode can adopt either a helical winding configuration or a transparent electrode architecture [61].

2.2. Preparation Process

The commercialization process of ACEL technology is greatly facilitated by the maturity of its open manufacturing processes. Unlike traditional semiconductor manufacturing that requires cleanroom environments, ACEL devices can be efficiently produced through various low-cost techniques. The fabrication of wearable ACEL devices follows the two structural paradigms of fiber and planar, each demanding distinct preparation methodologies. The fiber-based route constructs functional layers on individual fibers and weaves them into textiles, maximizing the softness and breathability of the fabric [65-67]. However, the central challenge lies in achieving continuous, uniform, and strong adhesion of functional materials on the curved fiber surface, while withstanding the mechanical stresses of subsequent weaving processes. This requirement imposes stringent demands on the interfacial adhesion, wear resistance, and encapsulation of the functional materials. The

planar-based route directly stacks functional layers on the surface of the fabric to form luminescent devices, exhibiting superior performance in image resolution, uniformity, patternability, and mechanical stability, facilitating the realization of complex graphics and versatile wearable forms [68,69]. It thus represents the current prevailing approach, offering an optimal balance between display performance and wearing experience.

For planar ACEL devices, spin coating [37,62,70-74] and screen printing [64,75-78] are the predominant preparation methods. While spin coating offers versatile thin-film deposition across a wide thickness range (nanometers to micrometers), it nonetheless struggles with uniform coating on flexible substrates and large-area continuous processing, hindering its direct use on fabrics (**Fig. 3(a)**) [62].

To overcome the shortcomings of spin coating, 3D printing technology has emerged as a solution that provides unprecedented design flexibility in the fabrication of ACEL devices (**Fig. 3(b)**) [43,79]. Multi-material printing systems enable precise spatial control over functional materials, facilitating three-dimensional integration of the luminescent, electrode, and packaging layers. However, its development is limited by the stringent ink requirements (such as viscosity and surface tension needing to be within narrow windows), and printing defects like the coffee ring effect and nozzle clogging. Moreover, the precision of alignment and interlayer interface quality control during multi-layer printing remain technical challenges.

Compared to the stringent ink requirements of printing technology, spray coating exhibits better process adaptability and scalability (**Fig. 3(c)**) [38,63,80]. The process is capable of employing low-viscosity inks and rapidly forming functional coatings over complex, uneven surfaces through adjustments to spray parameters, movement paths, and layered deposition, thus making it ideal for integration with flexible textiles and roll-to-roll mass production. However, the challenges of spray coating include controlling the film thickness uniformity, preventing edge blurring from spray mist, and overcoming its inherently lower material efficiency compared to printing. These factors may affect the consistency of device performance and image resolution.

Screen printing technology remains the mainstream method for mass production of ACEL devices, with the advantage of being able to complete the patterned deposition of multi-layer structures in one step and achieving material utilization rates of over 95% (**Fig. 3(d)**) [64,81,82]. The latest developments in high-resolution screen printing (with line widths reaching 20 μm) can meet the needs of most display applications, and adopting a roll-to-roll continuous printing method has further reduced production costs to one-tenth of traditional methods. However, the process lacks flexibility due to its reliance on solid screens, and the required high-viscosity slurries often cause clogging and defects, posing challenges when addressing applications requiring superior pattern fidelity.

Looking ahead, spray coating technology is expected to complement spin coating and screen printing, paving the way for high-performance, low-cost, and large-scale manufacturing of planar ACEL devices. Subsequent research should focus on three key objectives: developing environmentally friendly, thermally stable, and fabric-compatible functional inks; optimizing the spray coating process to achieve high-resolution patterns and stable interlayer structures; and systematically evaluating long-term reliability under real wearing conditions. These efforts are crucial for establishing the manufacturing standards for commercially produced ACEL devices.

When evaluating the aforementioned fabrication processes, their compatibility with high-performance materials and the economic feasibility of scale-up are key determinants of whether a technology can be industrialized. For example, the widely studied high-k composite dielectric barium titanate ($BaTiO_3$) [37], pursued to achieve high luminance, faces industrialization challenges such as the controllable, low-cost synthesis and surface modification of nanoscale $BaTiO_3$ powders, and the adverse effects of high filler loading on ink rheology and printing uniformity. Similarly, high-performance silver nanowire (AgNW) transparent electrodes are constrained in large-scale application by the high cost of silver, the stringent control required over nanowire aspect ratio and dispersibility, and the need for additional planarization or encapsulation layers to prevent migration and oxidation—factors that all increase process complexity and cost [41,74].

3. Composition and Materials of ACEL Devices

The typical flexible ACEL device can be regarded as a multilayer composite structure, with its performance core mainly relying on the synergistic effect of three functional layers: the luminescent layer, the dielectric layer, and the electrode layer [83,84]. The luminescent layer is usually composed of phosphor particles dispersed in a flexible polymer matrix, serving as the functional core for achieving electroluminescence. The dielectric layer encapsulates and protects the phosphor while playing a key role in distributing the electric field and preventing current breakdown. The electrode layer is responsible for injecting charge carriers and forming a flexible circuit, and it must possess excellent conductivity and mechanical flexibility. These three layers form an interdependent system where the material properties and structural design of each layer critically determine the device's overall performance, including its luminous efficiency, mechanical stability, and operational lifetime.

3.1. Phosphor

In flexible ACEL devices, the luminescent layer is a composite of phosphors dispersed within a polymer elastomer matrix, with its mechanical properties mainly determined by the polymer matrix and its luminescent characteristics dependent on the composition and structure of the selected phosphors [85-89]. Commonly used phosphors have an average particle size of about 25 μm. Although phosphors with smaller particle sizes (e.g., ≤ 9 μm [37,74]) enable a thinner luminescent layer and reduced operating voltage, their brightness and half-life are usually inferior, limiting their practical applications.

To regulate the luminescent color, various metal ions (e.g., Al^{3+} , Cu^{+} , Mn^{2+} , Ag^{+}) are often introduced into the phosphor matrix as activators. Under an electric field, these ions facilitate radiative recombination, and the distinct electronic energy level structures of each ion result in photons of specific energies. This mechanism produces a spectrum of emission colors spanning from blue and green to orange, and even white light. Furthermore, by incorporating multiple phosphors and modulating

their emission spectra, a wider range of multicolor luminescence and white light composite emission can be achieved [29,38,64,71].

3.2. Dielectric

In flexible ACEL devices, the selection of dielectric layer materials and structural design directly determines the device's stability, luminous efficiency, and operating voltage. High dielectric constant (high-k) materials improve insulation performance by suppressing electrical breakdown under high fields. Simultaneously, by regulating the distribution of the electric field within the luminescent layer, they enhance the effective electric field strength, thereby increasing luminous intensity and brightness. Currently, common high-k dielectric layer materials can be categorized into ceramic particle systems (e.g., $BaTiO_3$ [42,90,91]), polymer systems such as polyvinylidene fluoride (PVDF) [37,74,80,92], polydimethylsiloxane (PDMS) [93-95], thermoplastic polyurethane (TPU) [39,96], polyurethane (PU) [31,97], as well as their composites. The core of high-k dielectric material design lies in the synergistic optimization of dielectric constant, mechanical flexibility, and processability. Future trends include the development of ceramic/polymer core-shell structures [37], ionic gel composites [35], and self-healing dielectric materials [19,28,35] to simultaneously achieve high field coupling, excellent tensile properties, and long-term environmental stability.

3.2.1. Structure

In terms of structural design, ACEL devices can be divided into two main categories: those with an independent dielectric layer [80] and those without [44]. For devices with an independent dielectric layer, the dielectric layer and the fluorescent layer form a series of capacitor structure, and the distribution of the electric field between the two layers determines the field strength within the fluorescent layer. At this time, the dielectric layer can be considered as an insulator, whose primary function is to prevent current from directly flowing through the device and causing a short circuit, while effectively "coupling" the external alternating electric field to the

phosphors in the luminescent layer [98,99]. Under high electric fields, the dielectric layer can also store and release charges through displacement currents, limiting excessive current growth, thereby protecting the device and ensuring that the energy of the electric field is maximally used to excite the luminescent centers, achieving efficient luminescence.

In contrast, while the structure of devices without an independent dielectric layer (**Fig. 4(a)**) [44] is more straightforward for manufacturing and flexible integration, a significant mismatch in dielectric constants between the particles in the luminescent layer and the matrix (e.g., the combination of ZnS:Cu and PDMS) can lead to uneven local electric field distribution and a significant decrease in luminous efficiency. Therefore, how to achieve dielectric constant matching and optimize field distribution through material design has become a key issue for enhancing performance in structures without independent dielectric layers.

In addition, there is a blended system of dielectric fillers and luminescent powders that is worth noting (**Fig. 4(b)**) [37]. The core advantage of this blending strategy is that it can achieve a local reduction in device thickness while maintaining a relatively high dielectric constant [63,100], thereby allowing the luminescent layer to obtain a higher electric field strength in specific areas, which in turn results in higher local brightness and luminous efficiency [101,102]. Theoretically, such a system is beneficial for improving the effective field strength distribution in the luminescent layer and holds promise for further enhancing overall device performance when combined with existing high-k matrix materials or composite materials. However, the drawbacks of this blended system should not be overlooked. The blending of dielectric fillers and luminescent powders can lead to relative insufficient dispersion, inadequate interfacial interactions, and phenomena such as phase separation or agglomeration, causing uneven brightness distribution within the luminescent layer and possibly resulting in obvious brightness hotspots or dark areas. This uneven brightness affects visual uniformity and may adversely impact the reliability and lifespan of the device. Therefore, the design and preparation process must carefully control key parameters, including filler particle size distribution, surface modification,

the dispersing medium, and the blending ratio. Furthermore, advanced strategies such as interface coupling optimization, core-shell structures, or surface functionalization should be employed to enhance dispersion and interfacial consistency, thereby achieving a more uniform local electric field distribution and stable light output.

In conjunction with the aforementioned structural design, the dielectric filler/luminescent powder blended system can serve as a supplementary strategy for both types of devices, those with an independent dielectric layer and those without. In devices with an independent dielectric layer, blending expands the tunability of the dielectric environment of the luminescent layer. In devices without an independent dielectric layer, emphasis should be placed on addressing the uniformity of the blended phase and the consistency of local field distribution to avoid excessive local electric field gradients that could cause fluctuations in optical performance. Overall, the blended system of dielectric fillers and luminescent powders provides another important design pathway for the family of high-k dielectric materials, aiming to achieve higher luminous intensity and more flexible device structures by optimizing thickness and interfacial coupling under the premise of high dielectric constants. However, achieving highly uniform luminous output still requires in-depth optimization in material dispersion, compatibility, and processing techniques.

3.2.2. Materials

To overcome the aforementioned limitations, researchers are actively exploring the processing of high-k composite dielectric materials. The incorporation of $BaTiO_3$-based ceramic fillers in polymer matrices has shown significant performance improvements (**Fig. 4(c)**) [80]. For example, incorporating $BaTiO_3$ into a PDMS matrix can significantly enhance the brightness of devices, reaching several times that of traditional systems [103]. This effect is attributed to two aspects: first, the high-k fillers increase the dielectric constant of the composite material, thereby increasing the effective electric field in the fluorescent layer; second, through good dispersion and interfacial compatibility, the dielectric layer's capacity to withstand the electric

field and its breakdown strength are enhanced, allowing devices to achieve efficient light emission under lower applied electric fields.

In further exploration of material combinations, core-shell structured nanocomposites exhibit unique advantages. Guo et al. used $BaTiO_3$/PVP core-shell nanoparticles embedded in a PVDF-HFP elastomer to prepare nanocomposites with a dielectric constant exceeding 30 [37]. In such high-k core-shell systems, modifications to the filler surface and the presence of shell layers significantly reduce particle aggregation, enhance interfacial polarization effects, and maintain the flexibility and transparency of the matrix. Under approximately 35 V drive, devices made from these composites achieved a luminous brightness of about 116.7 cd/m², substantially exceeding the performance of the pure polymer control group and demonstrating the potential of composite structures in practical applications.

Shanker et al. conducted research from the perspective of material doping, achieving further enhancement of light emission performance through La-doped $BaTiO_3$ nanocubes [103]. Compared to undoped systems, the luminous brightness of the doped system increased by more than four times, indicating that ionic doping can effectively modulate the synergistic effects among lattice polarization response, interfacial polarization effects, and carrier injection/transmission characteristics. Such strategies, while improving dielectric constants, must also consider the potential impacts of doping on material lattice defects, scattering damage, and mechanical flexibility to ensure long-term reliability on flexible electronic substrates.

Another important category of high-k dielectric systems is the composites of ionic liquids and polymers [35]. Ionic liquids possess extremely high ionic conductivity and tunability, and when combined with polymer matrices, they can significantly improve the dielectric constant and control dielectric loss, while maintaining good mechanical flexibility [104,105]. However, the high ionic conductivity of ionic liquids also presents certain leakage risks and challenges in interfacial stability, which need to be effectively controlled through material design and packaging processes.

The strategies outlined above collectively form multiple pathways to enhance the performance of high-k dielectric layers. From the perspective of performance and application demands, the key design principles include: maximizing the effective dielectric constant and breakdown strength of the composite material while maintaining mechanical flexibility and transparency; reducing interfacial polarization losses and particle aggregation through interface engineering (e.g., core-shell coating, surface modification, doping); minimizing leakage current and addressing thermal stability issues while ensuring effective transport of electric field distribution to the light-emitting layer; and considering processing scalability, cost-effectiveness, and environmental compatibility. For structures with independent dielectric layers, the key to optimization lies in the precise control of dielectric layer thickness and interlayer compatibility, ensuring that the electric field in the fluorescent layer is enhanced without sacrificing the long-term stability and mechanical reliability of the device. For structures without independent dielectric layers, achieving a uniform distribution of field strength around the light-emitting particles through material matching and interface optimization is essential to avoid luminous efficiency loss caused by localized field weakening.

High-k dielectric materials can enhance the effective electric field within the emissive layer and help achieve a target luminance at lower drive voltages, thereby directly reducing power consumption. However, their dielectric loss (tan δ) must also be considered. Excessive dielectric loss causes most of the electrical energy to be dissipated as Joule heat rather than used to excite light, which significantly lowers the device's electroluminescent conversion efficiency and may introduce thermal-stability problems [105]. Therefore, the ideal dielectric design aims to increase k while minimizing loss as much as possible.

3.3. Electrodes

The performance and reliability of flexible ACEL devices largely depend on the comprehensive performance of their electrode systems. An ideal flexible electrode must simultaneously meet four key requirements: high electrical conductivity, high transmittance, excellent mechanical flexibility, and long-term environmental stability.

However, significant trade-offs exist among these criteria, presenting a fundamental challenge for technological advancement. Traditional indium tin oxide (ITO) electrodes exhibit nearly 90% transmittance and exceptional resistivity as low as 10^{-4} Ω·cm in rigid devices [106-108]. However, their intrinsic brittleness results in a fracture strain generally below 3%, making them prone to microcracks under mechanical deformation, leading to a sharp increase in resistance or even functional failure. This fundamental bottleneck makes it difficult for ITO to meet the durability and deformation requirements of future flexible electronic devices. The development of flexible electrodes is characterized by two major trends: hybridization and interface engineering. Ideal electrodes need to balance transparency, conductivity, flexibility, and stability. Future breakthroughs will rely on the design of metal nanowire/graphene hybrid structures [41], stretchable conductive gels [35], and bioinspired micro-structured electrodes, with a focus on resolving the electrical and mechanical coupling issues at the electrode-emissive layer interface under dynamic deformation.

To overcome the limitations of ITO, various electrode materials have been widely studied [111,112], each with unique advantages and challenges (**Fig. 5(a)**) [63]. Firstly, metal-based materials represented by AgNWs [41,74,113] and metal grids can achieve up to 90% transmittance and good bending resistance by controlling the diameter and surface density of the nanowires [114,115]. However, their surface roughness can easily lead to device short circuits, and the overlapping areas of the nanowires have a risk of contact failure under dynamic stress, necessitating reinforcement through surface planarization. Secondly, organic conductive polymers led by PEDOT:PSS have the significant advantage of excellent intrinsic flexibility (fracture strain > 30%) and compatibility with low-cost, solution-based fabrication [116-118]. However, their intrinsic conductivity is relatively low (typically 10^{-1}-10^{2} S/cm) and easily influenced by environmental humidity and temperature, limiting their application in devices that require high efficiency and long-term stability. In addition, carbon-based materials (**Fig. 5(b)**) [109], including graphene and carbon

nanotubes, theoretically offer extremely high transmittance, outstanding mechanical strength, and moderate conductivity [119-121]. Nonetheless, in practical applications, the high contact resistance between layers and inconsistent dispersion present significant challenges for commercialization.

Conventional electrodes, whether comprising silver nanowire grids, carbon nanotube networks [122], or patterned ITO, operate on the principle of electron transport through percolation networks. Regardless of how these materials are nanostructured or optimized for transparency, they inherently exhibit some degree of light absorption, reflection, or scattering, thereby imposing a fundamental upper limit on overall optical transmittance (**Fig. 5(c)**) [110]. In contrast, ionic gel electrodes operate through ion migration and consist of homogeneous, amorphous, continuous phases. The absence of internal solid nanostructures eliminates light-scattering interfaces, enabling near-ideal optical transparency approaching 100% (**Fig. 5(d)**) [35,123,124]. But ionic gels are associated with certain limitations, including slow response times and poor environmental stability, which currently restrict their application to scenarios requiring extreme mechanical deformability and high optical clarity. Notably, the long-term application of all flexible electrode candidates—whether metal nanowires, conductive polymers, or emerging ion gels—is primarily constrained by two common bottlenecks: inadequate dynamic mechanical stability and insufficient environmental durability [114,115]. Under repeated deformation, the microstructure of electrode materials (e.g., nanowire networks, polymer chain conformations) can evolve, leading to irreversible increases in resistance or even open circuits; meanwhile, ambient moisture, oxygen, and heat can accelerate electrode oxidation, degradation, or ion leakage. Therefore, evaluation of an electrode material must go beyond its initial conductivity and transparency and rigorously assess its stability under conditions that simulate real-world use (e.g., tens of thousands of bending cycles, high-temperature/high-humidity aging) [119].

In the future, synergistically complementing the advantages of different materials will become a mainstream direction. For example, embedding highly conductive silver nanowires into a flexible polymer matrix to form composite electrodes and

using graphene as an ultra-thin overlay to simultaneously achieve the planarization, protection, and performance enhancement of the AgNWs network. Additionally, research focus is shifting from the materials themselves to precise interface engineering, aiming to further enhance the overall efficiency, stability, and lifespan of devices by optimizing the interfacial properties between electrode, light-emitting layer, and encapsulation layer.

4. ACEL Display Devices

With the continuous development of flexible display technology, the evolution of display complexity can be clearly divided into three levels: static patterned displays [100,125,126], dynamic pixelated displays [127-129], and highly integrated display systems [130-132]. Together, these three levels drive the application potential of flexible ACEL displays in wearable, smart textiles, and flexible electronics. These levels represent a gradient in technological maturity. Static-pattern displays exhibit relatively high technological readiness and have been deployed in commercial signage and flexible backlighting. Dynamic pixelated displays [127] remain largely at the laboratory-prototype stage and require further optimization for high resolution and full-color operation. System-level integration examples (e.g., respiration-responsive masks, joint-motion monitoring) [45] are predominantly at the proof-of-concept stage and still face practical challenges in long-term stability, signal calibration, and system power consumption.

As shown in **Fig. 6(a)** [74], static patterned displays constitute the most fundamental level. Their core principle lies in the patterning treatment of a single electrode (usually the upper electrode), allowing the alternating electric field to be concentrated only in the overlapping area of the upper and lower electrodes, thereby achieving luminous patterns as preset [74]. This design approach is simple in principle and relatively reliable in process, accounting for its widespread adoption from early to recent implementations (**Fig. 6(b)**) [37]. A typical case is exemplified by the work of Zhou et al., who fabricated a butterfly-shaped top electrode from silver

nanowires, successfully creating a butterfly-patterned display that remains stable under a 40% stretching strain, demonstrating the reliability of static patterning in high-strain environments (**Fig. 6(c)**) [90]. The advantages of this approach include a simple structure, mature device fabrication processes, and strong pattern controllability, facilitating the rapid realization of specific visual effects or functional markings. Despite its advantages, the presented display pattern is fixed upon device fabrication and cannot be freely adjusted or switched afterward.

Dynamic pixelated displays rely on two mutually perpendicular patterned electrode layers. Their intersections form independent light-emitting pixels, creating an addressable pixel array. The core advantage of this structure is that it can theoretically achieve true pixel-level control, significantly enhancing display resolution and information capacity [64,135,136]. Shin et al. demonstrated an 8×8 large-area stretchable pixel array that can maintain uniform illumination under complex deformations such as bending and rolling, showcasing the robustness of pixelated displays during mechanical deformation (**Fig. 6(d)**) [36]. More importantly, the implementation of this strategy has expanded from planar film devices to fiber-like devices, greatly enhancing integration versatility and application potential.

To overcome the limitations of static displays, researchers have begun to integrate multiple independently controllable fixed patterns into a single device, marking an initial step towards dynamic pixelated displays. The core of this stage lies in increasing the number of independent control units, allowing the display area to have a variable number of light segments or even basic pixel-level control, while retaining fixed patterns as carriers [137]. Representative works include environmental sensing applications in wearable devices, such as the humidity-responsive interactive display (CUISD) based on dynamic ACEL developed by Pan et al. (**Fig. 6(e)**) [42]. By integrating highly responsive hydrogels into the ACEL layer, sub-second humidity-induced [133,138] luminescence has been achieved (**Fig. 6(f)**) [133]. A leading trend in pixelated display research is the shift toward fiber-based and textile-integrated systems. Patterned electrodes and light-emitting layers created

through electrospinning and microfabrication have formed large-scale (**Fig. 6(g)**) [39], high-resolution, multi-color, and dynamic displays (**Fig. 6(h)**) [134].

5. ACEL Interactive Integrated Applications

Flexible ACEL technology is undergoing a revolutionary transformation from a mere "information display" terminal to a multifunctional "interactive integrated" interface, becoming an intelligent medium that connects the human body, machines, and the physical world (**Fig. 7(a)**) [139]. Fig. 7(b)-7(g) systematically presents the evolution path of this technology from basic luminescent units to a comprehensive human-machine interaction system, showcasing the versatile integration of flexible ACEL devices in interactive displays.

Firstly, at the function level, the development of ACEL reflects a transition from passive display to active perception and feedback [139]. The visual-tactile feedback system presented in **Fig. 7(b)** shows that ACEL devices not only convey information through luminescence but also work in coordination with tactile actuators below [140,141]. When a user touches virtual buttons on the screen, localized backlight and vibration feedback appear synchronously, creating an immersive "what you see is what you touch" experience. This multimodal feedback enhances the interface's perceptibility, improving the intuitiveness and naturalness of interaction. Beyond interactive interfaces, the versatility of ACEL devices extends to physiological monitoring. As shown in **Fig. 7(c)**, flexible ACEL serves as a "smart skin" for joint activity tracking, where its luminance intensity and color shift recognizably in response to the bending angle [63]. This can transform physical movement into intuitive optical signals in real time, providing a new communicative dimension for non-verbal communication and expanding the expressive boundaries of human-machine interaction.

Secondly, at the system integration level, ACEL forms several independent yet cooperative intelligent service nodes through deep coupling with sensing and communication modules. The smart textile node demonstrated in **Fig. 7(d)** integrates distributed display units with micro-sensing capabilities into a display system. This

system not only displays the user's geographical information in real time but also facilitates the sending and receiving of messages and display between the user and a mobile phone. This capability highlights the broad prospects of ACEL displays in the fields of future wearable electronics and smart textiles [39]. The system in **Fig. 7(e)** integrates luminescent display, physiological sensing, and communication into a closed loop, representing a significant advance toward remote medical scenarios [46]. Leveraging wireless transmission and remote consultation, this system allows physicians to conduct diagnostics remotely. It establishes a comprehensive service system integrating monitoring, display, and communication, significantly improving the accessibility and quality of the remote medical experience [46].

Finally, at the holistic interconnection level, ACEL becomes a critical bridge connecting the virtual information world and the physical world, promoting the coordinated intelligence of "human-machine-object" systems. The wireless appliance control scenario in **Fig. 7(f)** allows users to interact with flexible panels integrated with ACEL through gestures or touch [45]. The panels provide intuitive visual feedback while directly sending control commands via wireless protocols such as Wi-Fi or Bluetooth, achieving seamless linkage between physical interfaces, digital displays, and IoT execution. This model greatly simplifies user operation paths, enhancing the fluency and responsiveness of the smart home experience. Furthermore, the interactive respiratory mask shown in **Fig. 7(g)** pushes human-machine integration to the extreme: ACEL displays dynamically change with respiratory frequency and intensity, transforming seemingly invisible vital signs into artistic visual expressions, offering physiological monitoring functions while enhancing the user's awareness of health status and emotional resonance on an emotional level [42].

6. Conclusion and Outlook

In this review, we systematically elaborate on the complete technological chain of flexible ACEL devices, from basic configurations to system integration. We first delve into their working mechanisms and analyze the design and performance characteristics of two typical device structures: thin-film and fiber-based. On this

basis, we provide a detailed review of the latest advancements in key material systems comprising these devices, including phosphors, high-k dielectric materials, and transparent conductive electrodes, which are crucial for constructing stretchable and conformally adherent light-emitting devices. Subsequently, we highlight the extensive applications of flexible ACEL devices as display and sensing platforms in cutting-edge fields. From the systematic overview provided in this review, it is clear that flexible ACEL technology has evolved from a basic lighting and display solution into a highly interdisciplinary research and innovation platform.

The practical implementation of flexible ACEL technology urgently requires coordinated efforts to overcome the following four challenges:

(1) Achieving high dielectric constant, low loss, and high flexibility simultaneously

Current high‐k dielectrics often sacrifice flexibility or incur higher loss when their permittivity is increased [105]. Future work must develop integrated "high‐k, low‐loss, highly flexible" composite materials. The key lies in synergistically tuning polarization characteristics and mechanical properties at the molecular and microscopic scales through approaches such as core–shell architectures, exploration of novel flexible ferroelectric polymers, or filler alignment techniques.

(2) Creating electrodes that are simultaneously highly conductive, highly transparent, and intrinsically stretchable

Existing electrodes struggle to combine high conductivity, high transparency, and large stretchability. Promising directions include multi‐mechanism hybrid bioinspired electrodes—for example, heterostructures composed of metal nanowires/2D materials/polymers—or elastic conductors based on liquid metals, coupled with precise interfacial mechanics design to maintain stable electrical connectivity under extreme deformation [60,61].

(3) Developing efficient and stable new organic–inorganic hybrid systems

Organic–inorganic hybrids offer a new materials dimension for high‐performance ACEL. Future work should explore photoluminescent hybrid materials—for instance, embedding highly efficient photoluminescent rare‐earth

complexes, organic dyes, or carbon dots into flexible inorganic matrices—and using the alternating electric field of the dielectric layer to indirectly excite luminescence. This indirect "field‐excitation to photon‐conversion" pathway could relax traditional ACEL requirements on material conductivity and open routes to low‐voltage, multimode light‐emitting device architectures [29,63], but core issues such as energy‐transfer efficiency, interface design, and long‐term photostability must be resolved.

(4) Developing low‐cost, high‐throughput manufacturing processes

Scalable production requires deep process–material integration. The core objective is to promote roll‐to‐roll (R2R) printing as the mainstream platform, which depends on developing functional inks suitable for high‐speed printing, solving large‐area film uniformity issues, and achieving low‐cost manufacturing of high‐performance devices [116,117].

Acknowledgements

This work is supported by the National Key R&D Program of China (2023YFA0915200), National Natural Science Foundation of China (grant numbers BE1100046, 21834007 and T2188102), Shanghai "Science and Technology Innovation Action Plan" Project (23JC1402900), Shanghai Pilot Program for Basic Research, National Research Foundation, Prime Minister's Office, Singapore under its Campus for Research Excellence and Technological Enterprise (CREATE) programme (CNSB) and Shanghai Jiao Tong University (grant numbers SD6040004/089 and WH220411004).

Conflict of Interest

All the contributing authors report no conflict of interests in this work.

Author contribution statement

K. X.: Methodology, investigation, writing – original draft. Y. Z. L., P. P. C.: Conceptualization, methodology, visualization, writing – review & editing. Z. T. Z.:

Supervision, funding acquisition, writing – review & editing. All the authors have approved the final manuscript.

Use of AI statement

None.

References

[1] Chen, X.; Lou, Z.; Gao, X.; Yin, L.; Qin, S.; Lin, M.; Zhang, F.; Lu, Y.; Ding, S.; Liu, R. et al. A noise-tolerant human–machine interface based on deep learning-enhanced wearable sensors. *Nat. Sens* **2025.**

[2] Zhang, Z.; Wang, Y.; Jia, S.; Fan, C. Body-conformable light-emitting materials and devices. *Nat. Photonics* **2023**, *18*, 114–126.

[3] Zhang, Z. Light-emitting materials for wearable electronics. *Nat. Rev. Mater.* **2022**, *7*, 839–840.

[4] Lin, Y.; Chen, X.; Lu, Q.; Wang, J.; Ding, C.; Liu, F.; Kong, D.; Yuan, W.; Su, W.; Cui, Z. Thermally laminated lighting textile for wearable displays with high durability. *ACS Appl. Mater. Interfaces* **2023**, *15*, 5931–5941.

[5] Kim, W.; Lee, K.; Choi, S.; Park, E.; Kim, G.; Ha, J.; Kim, Y.; Jang, J.; Oh, J. H.; Kim, H. et al. Electrochemiluminescent tactile visual synapse enabling in situ health monitoring. *Nat. Mater.* **2025**, *24*, 925–934.

[6] Wei, X. Y.; Liu, L.; Wang, H. L.; Kuang, S. Y.; Zhu, X.; Wang, Z. L.; Zhang, Y.; Zhu, G. High-intensity triboelectrification‐induced electroluminescence by microsized contacts for self‐powered display and illumination. *Adv. Mater. Interfaces* **2018**, *5*, 1701063.

[7] Wei, X.; Li, H.; Yue, W.; Gao, S.; Chen, Z.; Li, Y.; Shen, G. A high-accuracy, real-time, intelligent material perception system with a machine-learning-motivated pressure-sensitive electronic skin. *Matter* **2022**, *5*, 1481–1501.

[8] Song, S.; Song, B.; Cho, C.-H.; Lim, S. K.; Jeong, S. M. Textile-fiber-embedded multiluminescent devices: a new approach to soft display systems. *Mater. Today* **2020**, *32*, 46–58.

[9] Shi, J.; Liu, S.; Zhang, L.; Yang, B.; Shu, L.; Yang, Y.; Ren, M.; Wang, Y.; Chen, J.; Chen, W.; Chai, Y.; Tao, X. Smart textile-integrated microelectronic systems for wearable applications. *Adv. Mater.* **2020**, *32*, 1901958.

[10] Arwani, R. T.; Tan, S. C. L.; Sundarapandi, A.; Goh, W. P.; Liu, Y.; Leong, F. Y.; Yang, W.; Zheng, X. T.; Yu, Y.; Jiang, C.; Ang, Y. C. et al. Stretchable ionic-electronic bilayer hydrogel electronics enable in situ detection of solid-state epidermal biomarkers. *Nat. Mater.* **2024**, *23*, 1115–1122.

[11] Yang, X.; Chen, W.; Fan, Q.; Chen, J.; Chen, Y.; Lai, F.; Liu, H. Electronic skin for health monitoring systems: properties, functions, and applications. *Adv. Mater.* **2024**, *36*, 2402542.

[12] Ni, Y.; Zang, X.; Yang, Y.; Gong, Z.; Li, H.; Chen, J.; Wu, C.; Huang, J.; Lai, Y. Monitoring with ultrahigh sensitivity. *Adv. Funct. Mater.* **2024**, *34*, 2402853.

[13] Sun, Y.; Zhu, L.; Yang, J.; Zhang, J.; Chen, B.; Wang, Z. L. Flexible alternating-current electroluminescence plunging to below 1 Hz frequency by triboelectrification. *Adv. Opt. Mater.* **2021**, *10*, 2101918.

[14] He, J.; Lu, C.; Jiang, H.; Han, F.; Shi, X.; Wu, J.; Wang, L.; Chen, T.; Wang, J.; Zhang, Y. et al. Scalable production of high-performing woven lithium-ion fibre batteries. *Nature* **2021**, *597*, 57–63.

[15] Yang, C. H.; Chen, B.; Zhou, J.; Chen, Y. M.; Suo, Z. Electroluminescence of giant stretchability. *Adv. Mater.* **2015**, *28*, 4480–4484.

[16] Chen, Y.; Xia, Y.; Smith, G. M.; Carroll, D. L. Frequency-dependent, alternating current - driven, field-induced polymer electroluminescent devices with high power efficiency. *Adv. Mater.* **2014**, *26*, 8133–8140.

[17] Wang, J.; Yan, C.; Cai, G.; Cui, M.; Lee-Sie Eh, A.; See Lee, P. Extremely stretchable electroluminescent devices with ionic conductors. *Adv. Mater.* **2015**, *28*, 4490–4496.

[18] Sun, J.; Chang, Y.; Dong, L.; Zhang, K.; Hua, Q.; Zang, J.; Chen, Q.; Shang, Y.; Pan, C.; Shan, C. MXene enhanced self-powered alternating current electroluminescence devices for patterned flexible displays. *Nano Energy* **2021**, *86*, 106077.

[19] Chang, Y.; Sun, J.; Dong, L.; Jiao, F.; Chang, S.; Wang, Y.; Liao, J.; Shang,

Y.; Wu, W.; Qi, Y. et al. Self-powered multi-color display based on stretchable self-healing alternating current electroluminescent devices. *Nano Energy* **2022**, *95*, 107061.

[20] Jayathilaka, W. A. D. M.; Chinnappan, A.; Ji, D.; Ghosh, R.; Tran, T. Q.; Ramakrishna, S. Facile and scalable electrospun nanofiber-based alternative current electroluminescence (ACEL) device. *ACS Appl. Electron. Mater.* **2021**, *3*, 267–276.

[21] Vellaichamy, M.; Jagodič, U.; Pišljar, J.; Zaplotnik, J.; Mur, U.; Jelen, A.; Nych, A.; Malkar, D.; Ryzhkova, A. V.; Škarabot, M. et al. Microscale generation and control of nanosecond light by light in a liquid crystal. *Nat. Photonics* **2025**, *19*, 758–766.

[22] Zhang, Q.; Li, B.; Huang, S.; Nomura, H.; Tanaka, H.; Adachi, C. Efficient blue organic light-emitting diodes employing thermally activated delayed fluorescence. *Nat. Photonics* **2014**, *8*, 326–332.

[23] Song, H.; Song, Y. J.; Hong, J.; Kang, K. S.; Yu, S.; Cho, H.-E.; Kim, J.-H.; Lee, S.-M. Water stable and matrix addressable OLED fiber textiles for wearable displays with large emission area. *npj Flexible Electron.* **2022**, *6*, 66.

[24] Li, R.; Wang, Y.; Chen, Y.; Zhao, J.; Wang, Y.; An, J.; Lu, Y.; Chen, Y.; Lai, W.; Zhang, X. et al. Efficient flexible fabric-based top-emitting polymer light-emitting devices for wearable electronics. *Small* **2023**, *20*, 2305327.

[25] Wu, Z.; Ma, D. Recent advances in white organic light-emitting diodes. *Mater. Sci. Eng.: R: Rep.* **2016**, *107*, 1–42.

[26] Wood, V.; Halpert, J. E.; Panzer, M. J.; Bawendi, M. G.; Bulović, V. Alternating current driven electroluminescence from ZnSe/ZnS:Mn/ZnS nanocrystals. *Nano Lett.* **2009**, *9*, 2367–2371.

[27] Wang, J.; Yan, C.; Chee, K. J.; Lee, P. S. Highly stretchable and self-deformable alternating current electroluminescent devices. *Adv. Mater.* **2015**, *27*, 2876–2882.

[28] Cho, S. H.; Lee, S. W.; Hwang, I.; Kim, J. S.; Jeong, B.; Kang, H. S.; Kim, E. H.; Kim, K. L.; Park, C.; Park, C. Shape-deformable self-healing electroluminescence displays. *Adv. Opt. Mater.* **2019**, *7*, 1801283.

[29] Wang, X.; Lin, Y.; Zhang, Y.; Xu, S.; Liu, M.; Shen, Y.; Gong, Y.; Xiong, Y.; Hu, Y. Coplanar pattern and temperature transient control in intelligent wearable multi-color alternating current electroluminescence devices. *Adv. Funct. Mater.* **2025**, *35*, 2420613.

[30] Su, L.; Wang, Z.;Lu, C.; Ding, W.; Zhao, Y.; Zi, Y. Persistent triboelectrification-induced electroluminescence for self-powered all-optical wireless user identification and multi-mode anti-counterfeiting. *Mater. Horiz.* **2023**, *10*, 2445–2454.

[31] Li, G.; Sun, F.; Zhao, S.; Xu, R.; Wang, H.; Qu, L.; Tian, M. Autonomous electroluminescent textile for visual interaction and environmental warning. *Nano Lett.* **2023**, *23*, 8436–8444.

[32] Liu, X.; Zhang, M.; Yang, Z.; Wang, H.; Chen, J.; Wang, Z.; Lu, Y.; Chen, Y.; Ji, L.; Cheng, J. Alternating current electroluminescent device powered by triboelectric nanogenerator with capacitively driven circuit strategy. *Adv. Funct. Mater.* **2021**, *32*, 2106411.

[33] Wang, L.; Xiao, L.; Gu, H.; Sun, H. Advances in alternating current electroluminescent devices. *Adv. Opt. Mater.* **2019**, *7*, 1801154.

[34] Jayathilaka, W. A. D. M.; Chinnappan, A.; Tey, J. N.; Wei, J.; Ramakrishna, S. Alternative current electroluminescence and flexible light emitting devices. *J. Mater. Chem. C* **2019**, *7*, 5553–5572.

[35] Liu, Y.; Sun, L.; Feng, W.; Jin, Z.; Wang, C. A stable, self-healable, and stretchable dielectric polymer for electroluminescent device working underwater. *Adv. Funct. Mater.* **2024**, *34*, 2402453.

[36] Shin, H.; Sharma, B. K.; Lee, S. W.; Lee, J.-B.; Choi, M.; Hu, L.; Park, C.; Choi, J. H.; Kim, T. W.; Ahn, J.-H. Stretchable electroluminescent display enabled by graphene-based hybrid electrode. *ACS Appl. Mater. Interfaces*

2019, *11*, 14222–14228.

[37] Zhou, Y.; Zhao, C.; Wang, J.; Li, Y.; Li, C.; Zhu, H.; Feng, S.; Cao, S.; Kong, D. Stretchable high-permittivity nanocomposites for epidermal alternating-current electroluminescent displays. *ACS Mater. Lett.* **2019**, *1*, 511–518.

[38] Luo, Z.; Chen, W.; Lai, M.; Shi, S.; Chen, P.; Yang, X.; Chen, Z.; Wang, B.; Zhang, Y.; Zhou, X. Fully printable and reconfigurable hufu-type electroluminescent devices for visualized encryption. *Adv. Mater.* **2024**, *36*, 2313909.

[39] Shi, X.; Zuo, Y.; Zhai, P.; Shen, J.; Yang, Y.; Gao, Z.; Liao, M.; Wu, J.; Wang, J.; Xu, X. et al. Large-area display textiles integrated with functional systems. *Nature* **2021**, *591*, 240–245.

[40] Qu, C.; Xu, Y.; Xiao, Y.; Zhang, S.; Liu, H.; Song, G. Multifunctional displays and sensing platforms for the future: A review on flexible alternating current electroluminescence devices. *ACS Appl. Electron. Mater.* **2021**, *3*, 5188–5210.

[41] You, B.; Kim, Y.; Ju, B.-K.; Kim, J.-W. Highly stretchable and waterproof electroluminescence device based on superstable stretchable transparent electrode. *ACS Appl. Mater. Interfaces* **2017**, *9*, 5486–5494.

[42] He, J.; Wei, R.; Ma, X.; Wu, W.; Pan, X.; Sun, J.; Tang, J.; Xu, Z.; Wang, C.; Pan, C. Contactless user-interactive sensing display for human-human and human-machine interactions. *Adv. Mater.* **2024**, *36*, 2401931.

[43] Zhang, P.; Lei, I. M.; Chen, G.; Lin, J.; Chen, X.; Zhang, J.; Cai, C.; Liang, X.; Liu, J. Integrated 3D printing of flexible electroluminescent devices and soft robots. *Nat. Commun.* **2022**, *13*, 4775.

[44] Tan, Y. J.; Godaba, H.; Chen, G.; Tan, S. T. M.; Wan, G.; Li, G.; Lee, P. M.; Cai, Y.; Li, S.; Shepherd, R. F. et al. A transparent, self-healing and high-κ dielectric for low-field-emission stretchable optoelectronics. *Nat. Mater.* **2019**, *19*, 182–188.

[45] Yang, W.; Lin, S.; Gong, W.; Lin, R.; Jiang, C.; Yang, X.; Hu, Y.; Wang, J.; Xiao, X.; Li, K.; Li, Y. et al. Single body-coupled fiber enables chipless textile electronics. *Science* **2024**, *384*, 74–81.

[46] Li, Y.; Lin, Q.; Sun, T.; Qin, M.; Yue, W.; Gao, S. A perceptual and interactive integration strategy toward telemedicine healthcare based on electroluminescent display and triboelectric sensing 3D stacked device. *Adv. Funct. Mater.* **2024**, *34*, 2402356.

[47] Chen, F.; Kitai, A. H. Application of indium nanowires to donor–acceptor pair luminescence. *J. Lumin.* **2008**, *128*, 1856–1862.

[48] Smet, P. F.; Moreels, I.; Hens, Z.; Poelman, D. Luminescence in sulfides: a rich history and a bright future. *Materials* **2010**, *3*, 2834–2883.

[49] Xie, Q.; Yao, Y.; Wu, L.; Xue, Y.; Shen, G.; Guo, C.; Du, B.; Wu, H.; Jin, Y. Design principles of electroluminescent devices based on different electrodes and recent advances toward their application in textiles. *J. Mater. Chem. C* **2025**, *13*, 8934–8957.

[50] Rastogi, C. K.; Mishra, R. K.; Chirauri, S.; Rao, K. R.; Vatsa, R. K.; Kadam, R. M.; Sudarsan, V. Comparative study on photo and electroluminescence properties of Cu-doped ZnS. *Physica B* **2022**, *640*, 414054.

[51] Li, J.; Zhang, Z.; Luo, X.; Zhu, L.; Wang, Z. L. Triboelectric leakage-field-induced electroluminescence based on ZnS:Cu. *ACS Appl. Mater. Interfaces* **2022**, *14*, 4775–4782.

[52] Lin, C.; Yang, R.; Wu, Z.; Wang, Y.; Zhan, C.; Miyata, H.; Zeng, X.; Zheng, Y.; You, S.; Lv, Y. et al. Ueda, J. Electrically chargeable inorganic persistent luminescence in an alternating current driven electroluminescent device. *Commun. Mater.* **2025**, *6*, 25.

[53] Hikmet, R. A. M.; Talapin, D. V.; Weller, H. Study of conduction mechanism and electroluminescence in CdSe/ZnS quantum dot composites. *J. Appl. Phys.* **2003**, *93*, 3509–3514.

[54] Lee, C.-W.; Schleife, A. Hot-Electron-Mediated Ion Diffusion in

Semiconductors for Ion-Beam Nanostructuring. *Nano Lett.* **2019**, *19*, 3939–3947.

[55] Fischer, A. G. Electroluminescent lines in ZnS powder particles: II . models and comparison with experience. *J. Electrochem. Soc.* **1963**, *110*, 733.

[56] Fischer, A. G. Electroluminescent lines in ZnS powder particles: I . embedding media and basic observations. *J. Electrochem. Soc.* **1962**, *109*, 1043.

[57] Hu, B.; Li, D.; Ala, O.; Manandhar, P.; Fan, Q.; Kasilingam, D.; Calvert, P. D. Textile-based flexible electroluminescent devices. *Adv. Funct. Mater.* **2010**, *21*, 305–311.

[58] Liang, G.; Yi, M.; Hu, H.; Ding, K.; Wang, L.; Zeng, H.; Tang, J.; Liao, L.; Nan, C.; He, Y. et al. Coaxial-structured weavable and wearable electroluminescent fibers. *Adv. Electron. Mater.* **2017**, *3*, 1700401.

[59] Lv, S.; Han, Y.; Shuai, L.; Chen, B.; Wan, J. ZFP+PU/PVDF composite fibers based on ZnS:Cu phosphors for low temperature lighting monitoring sensor devices. *J. Lumin.* **2021**, *239*, 118303.

[60] Wang, Z.; Tai, Y.; Ye, Z.; Nam, J.; Yin, Y. Integration of ZnS: Mn^{2+} microparticles into electrospun PVDF-based nanofibers for enhanced mechanoluminescence. *Adv. Funct. Mater.* **2024**, *34*, 2410358.

[61] Mi, H.; Zhong, L.; Tang, X.; Xu, P.; Liu, X.; Luo, T.; Jiang, X. Electroluminescent fabric woven by ultrastretchable fibers for arbitrarily controllable pattern display. *ACS Appl. Mater. Interfaces* **2021**, *13*, 11260–11267.

[62] Wang, C.; Gao, B.; Xue, K.; Wang, W.; Zhao, J.; Bai, R.; Yun, T; Fan, Z.; Yang, M.; Zhang, Z. Stretchable [2]rotaxane-bridged MXene films applicable for electroluminescent devices. *Sci. Adv.* **2025**, *11*, eadt8262.

[63] Zhu, S.; Xiong, F.; Gu, Y.; Chen, W.; Fan, Q.; Lu, H.; Wang, T.; Yang, B.-R.; Deng, S. Low driving voltage electroluminescence device for integrated visual strain sensing. *ACS Appl. Mater. Interfaces* **2024**, *16*,

31657–31665.

[64] Zhao, C.; Zhou, Y.; Gu, S.; Cao, S.; Wang, J.; Zhang, M.; Wu, Y.; Kong, D. Fully screen-printed, multicolor, and stretchable electroluminescent displays for epidermal electronics. *ACS Appl. Mater. Interfaces* **2020**, *12*, 47902–47910.

[65] Yu, X.; Chen, L.; Zhang, J.; Yan, W.; Hughes-Riley, T.; Cheng, Y.; Zhu, M. Structural design of light-emitting fibers and fabrics for wearable and smart devices. *Sci. Bull.* **2024**, *69*, 2439–2455.

[66] Li, G.; Li, M.; Zhang, X.; Xu, R.; Liu, S.; Xu, T.; Tian, M. Stimulus-responsive alternating current electroluminescent textiles for visual human-machine interface. *Device* **2025**, *3*.

[67] Hu, X.; Zhang, B.; You, C.; Tian, M.; Xing, D.; Zhang, X.; Qu, L. Non-noble metal electroluminescent fibers for visual monitoring and interaction. *Adv. Fiber Mater.* **2025**, *7*, 227–239.

[68] Fu, P.; Li, J.; Zhong, M.; Huang, J.; Tan, R.; Song, W. Bendable and curlable electroluminescent devices based on roomtemperature deposited flexible indium zinc tin oxide electrode. *ACS Appl. Opt. Mater.* **2024**, *2*, 816–824.

[69] Sagar, P. & Kumar, B. PANI-reinforced-ZnS/PDMS-based flexible hybrid piezo-triboelectric nanogenerator for self-powered wearable electronics and sensing. *Mater. Res. Bull.* **2025**, *190*, 113482.

[70] Yang, M.; Wang, W.; Xue, K.; Gao, B.; Qu, S.; Fan, Z. W.; Wang, Y.; Yang, L.; Zhang, Z.; Yan, X. et al. Orthogonal yet synergistic supramolecular interactions to boost material properties. *Macromolecules* **2025**.

[71] Zuo, Y.; Shi, X.; Zhou, X.; Xu, X.; Wang, J.; Chen, P.; Sun, X.; Peng, H. Flexible color-tunable electroluminescent devices by designing dielectric-distinguishing double-stacked emissive layers. *Adv. Funct. Mater.* **2020**, *30*, 2005200.

[72] Wu, Y.; Mechael, S. S.; Lerma, C.; Carmichael, R. S.; Carmichael, T. B.

Stretchable ultrasheer fabrics as semitransparent electrodes for wearable light-emitting e-textiles with changeable display patterns. *Matter* **2020**, *2*, 882–895.

[73] Dai, C.; Wang, Y.; Shan, Y.; Ye, C.; Lv, Z.; Yang, S.; Cao, L.; Ren, J.; Yu, H.; Liu, S. et al. Cytoskeleton-inspired hydrogel ionotronics for tactile perception and electroluminescent display in complex mechanical environments. *Mater. Horiz.* **2023**, *10*, 136–148.

[74] Guo, H.; Lin, Y.; Gu, S.; Hu, G.; Wang, Q.; Bai, C.; Sun, Y.; Yang, C.; Fang, T.; Chen, X. et al. Stretchable and breathable electroluminescent displays based on ultrathin nanocomposite designs. *Nano Lett.* **2024**, *24*, 5904–5912.

[75] Yakoh, A.; Álvarez-Diduk, R.; Chailapakul, O.; Merkoçi, A. Screen-printed electroluminescent lamp modified with graphene oxide as a sensing device. *ACS Appl. Mater. Interfaces* **2018**, *10*, 20775–20782.

[76] Janczak, D.; Zych, M.; Raczyński, T.; Dybowska-Sarapuk, Ł.; Pepłowski, A.; Krzemiński, J.; Sosna-Głębska, A.; Znajdek, K.; Sibiński, M.; Jakubowska, M. Stretchable and washable electroluminescent display screen-printed on textile. *Nanomaterials* **2019**, *9*, 1276.

[77] Yakoh, A.; Siangproh, W.; Chailapakul, O.; Ngamrojanavanich, N. Optical bioelectronic device based on a screen-printed electroluminescent transducer. *ACS Appl. Mater. Interfaces* **2020**, *12*, 22543–22551.

[78] Gu, S.; Zhou, Y.; Li, Y.; Ma, T.; Guo, R.; Lu, Q.; Zhang, J.; Cao, S.; Zhu, H.; Li, D. et al. Ultrastretchable alternating current electroluminescent panels for arbitrary luminous patterns. *Appl. Mater. Today* **2023**, *31*, 101764.

[79] Cao, L.; Wang, Z.; Hu, D.; Dong, H.; Qu, C.; Zheng, Y.; Yang, C.; Zhang, R.; Xing, C.; Li, Z. et al. Pressure-constrained sonication activation of flexible printed metal circuit. *Nat. Commun.* **2024**, *15*, 8324.

[80] Zhang, Y.; Wang, X.; Zhang, Y.; Liu, M.; Zhao, Z.; Shen, Z.; Hu, Y. Wearable alternating current electroluminescent e-textiles with high

brightness enabled by fully sprayed layer-by-layer assembly. *Adv. Funct. Mater.* **2023**, *34*, 2308969.

[81] Yang, M.; Li, C.; Ni, H.; Song, Y.; Sun, J. Direct-write printed flexible, transparent, multicolor electroluminescent display with alternating-current electroluminescence ink. *ACS Appl. Mater. Interfaces* **2025**, *17*, 39330–39339.

[82] Park, J.; Singh, S.; Yoon, J. 3D printing of deformable multicolor alternating-current electroluminescent devices through rational design of functional inks. *Small* **2025**, *21*, 2502435.

[83] Yin, H.; Zhu, Y.; Youssef, K.; Yu, Z.; Pei, Q. Structures and materials in stretchable electroluminescent devices. *Adv. Mater.* **2022**, *34*, 2106184.

[84] Liu, Y.; Xu, M.; Long, H.; Vasiliev, R. B.; Li, S.; Meng, H.; Chang, S. Alternating current electroluminescence devices: recent advances and functional applications. *Mater. Horiz.* **2024**, *11*, 5147–5180.

[85] Xu, Y.; Chen, J.; Zhang, H.; Wei, H.; Zhou, L.; Wang, Z.; Pan, Y.; Su, X.; Zhang, A.; Fu, J. White-light-emitting flexible display devices based on double network hydrogels crosslinked by YAG:Ce phosphors. *J. Mater. Chem. C* **2020**, *8*, 247–252.

[86] Bhargava, R. N.; Gallagher, D.; Hong, X.; Nurmikko, A. Optical properties of manganese-doped nanocrystals of ZnS. *Phys. Rev. Lett.* **1994**, *72*, 416–419.

[87] Van, B. H.; Ben, P. V.; Thi, T. M.; Nhat, H. N. Absorption and radiation transitions in $Mn^{2+}(3d^5)$ configuration of Mn-doped ZnS nanoparticles synthesized by a hydrothermal method. *Journal of Materials* **2013**, *2013*, 716452.

[88] Xu, S. J.; Chua, S. J.; Liu, B.; Gan, L. M.; Chew, C. H.; Xu, G. Q. Luminescence characteristics of impurities-activated ZnS nanocrystals prepared in microemulsion with hydrothermal treatment. *Appl. Phys. Lett.* **1998**, *73*, 478–480.

[89] Lee, S.; Song, D.; Kim, D.; Lee, J.; Kim, S.; Park, I. Y.; Choi, Y. D. Effects of synthesis temperature on particle size/shape and photoluminescence characteristics of ZnS:Cu nanocrystals. *Mater. Lett.* **2004**, *58*, 342–346.

[90] Stauffer, F.; Tybrandt, K. Bright stretchable alternating current electroluminescent displays based on high permittivity composites. *Adv. Mater.* **2016**, *28*, 7200–7203.

[91] Son, Y. H.; Kim, S. J.; Kim, Y. M.; Jang, G. E.; Yoon, M. S.; Ur, S. C.; Ryu, S. L.; Kweon, S. Y. Characteristics of $BaTiO_3$-PVDF composite film for inorganic electro-luminescence device. *Integr. Ferroelectr.* **2010**, *98*, 183–191.

[92] Jayathilaka, W. A. D. M.; Chinnappan, A.; Ji, D.; Ghosh, R.; Tran, T. Q.; Ramakrishna, S. Facile and scalable electrospun nanofiber-based alternative current electroluminescence (ACEL) device. *ACS Appl. Electron. Mater.* **2020**, *3*, 267–276.

[93] von Szczepanski, J.; Wolf, J.; Hu, W. H.; Schneider, R.; Danner, P. M.; Kupferschmid, A.; Jenatsch, S.; Hany, R.; Nüesch, F. A.; Opris, D. M. High-permittivity polysiloxanes for bright, stretchable electroluminescent devices. *Adv. Opt. Mater.* **2024**, *12*, 2400132.

[94] Zhang, X.; Liu, C.; Shan, J.; Li, Z.; Guo, X.; Zhao, X.; Ding, J.; Yang, H. Flexible electroluminescent device based on ZnS:Cu-polyurethane composite and silver nanowires. *J. Mater. Sci.: Mater. Electron.* **2024**, *35*, 123.

[95] Sohn, K.-S.; Timilsina, S.; Singh, S. P.; Choi, T.; Kim, J. S. Mechanically driven luminescence in a ZnS:Cu-PDMS composite. *APL Mater.* **2016**, *4*, 106102.

[96] Cho, S.; Chang, T.; Yu, T.; Gong, S. L.; Lee, C. H. Machine embroidery of light-emitting textiles with multicolor electroluminescent threads. *Sci. Adv.*, *10*, eadk4295.

[97] Lu, H.; Zhang, Y.; Zhu, M.; Li, S.; Liang, H.; Bi, P.; Wang, S.; Wang, H.;

Gan, L.; Wu, X.-E. et al. Intelligent perceptual textiles based on ionic-conductive and strong silk fibers. *Nat. Commun.* **2024**, *15*, 3289.

[98] Wang, Z.; Song, X.; Chen, Q.; Liang, J.; Tu, Z.; Wang, C.; Zhang, Z.; Bi, H.; Wang, Y. Unveiling the aging process of organic light-emitting devices with langevin and hole trap-assisted recombination exciplex cohosts. *Adv. Funct. Mater.* **2022**, *32*, 2206207.

[99] Riley, D. B.; Sandberg, O. J.; Zarrabi, N.; Kim, Y. R.; Meredith, P.; Armin, A. Efficient nanoscale exciton transport in non-fullerene organic solar cells enables reduced bimolecular recombination of free charges. *Adv. Mater.* **2023**, *35*, 2211174.

[100] Ma, R.; Sun, Z.; Hao, Y.; Wang, T.; Guan, S.; Han, L.; Liu, R.; Jiao, S.; Liu, Y.; Zhou, Y. Alternating current electroluminescent (ACEL) devices for dynamic intelligent displays controlled by wireless networks. *ACS Appl. Electron. Mater.* **2025**.

[101] Zhao, C.; Yang, B.; Ali, M. U.; Zhao, Y.; Zhang, C.; Yin, Y.; Liu, M.; Yan, C.; Meng, H. Bright stretchable white alternating-current electroluminescent devices enabled by photoluminescent phosphor. *Adv. Mater. Technol.* **2022**, *7*, 2101440.

[102] Li, J.; Lin, Y.; Zhou, D.; Zhang, S.; Yuan, W.; Su, W.; Meng, X.; Wu, X.; Chi, C.; Kong, D. et al. High-brightness low voltage alternative current electroluminescent devices for human wearable displays. *Opt. Laser Technol.* **2025**, *184*, 112568.

[103] Shanker, R.; Cho, S.; Choe, A.; Kim, M. P.; Khan, Z.; Kang, S.; Ko, H. Solution-processable, high-performance flexible electroluminescent devices based on high-k nanodielectrics. *Adv. Funct. Mater.* **2019**, *29*, 1904377.

[104] Zhang, G.; Guo, Y.; Fang, Y.; Chu, Y.; Liu, Z. A wearable alternating current electroluminescent device based on imidazole chloride ionogel films with high conductivity, stretchability and transmittance. *J. Mater. Chem. C* **2023**, *11*, 5882–5889.

[105] Zhang, C.; Bao, Q.; Zhu, H.; Zhang, Q. Highly transparent and long-term stable dielectric elastomer composites enabled by poly(ionic liquid) inclusion. *Adv. Funct. Mater.* **2024**, *34*, 2401901.

[106] Aydın, E. B.; Sezgintürk, M. K. Indium tin oxide (ITO): a promising material in biosensing technology. *TrAC, Trends Anal. Chem.* **2017**, *97*, 309–315.

[107] Shigesato, Y.; Koshi-ishi, R.; Kawashima, T.; Ohsako, J. Early stages of ITO deposition on glass or polymer substrates. *Vacuum* **2000**, *59*, 614–621.

[108] Granqvist, C. G.; Hultåker, A. Transparent and conducting ITO films: new developments and applications. *Thin Solid Films* **2002**, *411*, 1–5.

[109] Nie, B.; Li, X.; Wang, C.; Liu, H.; Tian, H.; Chen, X.; Shao, J. Flexible double-sided light-emitting devices based on transparent embedded interdigital electrodes. *ACS Appl. Mater. Interfaces* **2020**, *12*, 43892–43900.

[110] Lee, S.; Kim, E. H.; Yu, S.; Kim, H.; Park, C.; Lee, S. W.; Han, H.; Jin, W.; Lee, K.; Lee, C. E. et al. Polymer-laminated $Ti_3C_2T_X$ MXene electrodes for transparent and flexible field-driven electronics. *ACS Nano* **2021**, *15*, 8940–8952.

[111] Ma, S.; Peng, Z.; Kitai, A. H. A CuO nanowire-based alternating current oxide powder electroluminescent device with high stability. *Angew. Chem. Int. Ed.* **2018**, *57*, 11267–11272.

[112] Jun, S.; Kim, Y.; Ju, B.-K.; Kim, J.-W. Extremely flexible, transparent, and strain-sensitive electroluminescent device based on ZnS:Cu-polyvinyl butyral composite and silver nanowires. *Appl. Surf. Sci.* **2018**, *429*, 144–150.

[113] Zhang, T.; Yang, P.; Li, Y.; Cao, Y.; Zhou, Y.; Chen, M.; Zhu, Z.; Chen, W.; Zhou, X. Flexible transparent sliced veneer for alternating current electroluminescent devices. *ACS Sustainable Chem. Eng.* **2019**, *7*, 11464–11473.

[114] Hu, L.; Kim, H. S.; Lee, J.-Y.; Peumans, P.; Cui, Y. Scalable coating and

properties of transparent, flexible, silver nanowire electrodes. *ACS Nano* **2010**, *4*, 2955–2963.

[115] Zeng, X.-Y.; Zhang, Q.-K.; Yu, R.-M.; Lu, C.-Z. A new transparent conductor: silver nanowire film buried at the surface of a transparent polymer. *Adv. Mater.* **2010**, *22*, 4484–4488.

[116] Lee, C. S.; Kim, J. Y.; Lee, D. E.; Joo, J.; Wagh, B. G.; Han, S.; Beag, Y. W.; Koh, S. K. Flexible and transparent organic film speaker by using highly conducting PEDOT/PSS as electrode. *Synth. Met.* **2003**, *139*, 457–461.

[117] Crispin, X.; Jakobsson, F. L. E.; Crispin, A.; Grim, P. C. M.; Andersson, P.; Volodin, A.; van Haesendonck, C.; Van der Auweraer, M.; Salaneck, W. R.; Berggren, M. The origin of the high conductivity of poly(3,4-ethylenedioxythiophene)-poly(styrenesulfonate) (PEDOT-PSS) plastic electrodes. *Chem. Mater.* **2006**, *18*, 4354–4360.

[118] Chang, H.; Wang, G.; Yang, A.; Tao, X.; Liu, X.; Shen, Y.; Zheng, Z. A transparent, flexible, low-temperature, and solution-processible graphene composite electrode. *Adv. Funct. Mater.* **2010**, *20*, 2893–2902.

[119] Ando, T. The electronic properties of graphene and carbon nanotubes. *NPG Asia Mater.* **2009**, *1*, 17–21.

[120] Liu, W.-W.; Chai, S.-P.; Mohamed, A. R.; Hashim, U. Synthesis and characterization of graphene and carbon nanotubes: a review on the past and recent developments. *J. Ind. Eng. Chem.* **2014**, *20*, 1171–1185.

[121] Kolahdouz, M.; Xu, B.; Nasiri, A. F.; Fathollahzadeh, M.; Manian, M.; Aghababa, H.; Wu, Y.; Radamson, H. H. Carbon-related materials: graphene and carbon nanotubes in semiconductor applications and design. *Micromachines.* **2022**, *13*, 1257.

[122] Wen, L.; Liu, N.; Wang, S.; Zhang, H.; Zhao, W.; Yang, Z.; Wang, Y.; Su, J.; Li, L.; Long, F. et al. Enhancing light emission in flexible AC electroluminescent devices by tetrapod-like zinc oxide whiskers. *Opt. Express* **2016**, *24*, 23419-23428.

[123] Wang, H.; Wang, Z.; Yang, J.; Xu, C.; Zhang, Q.; Peng, Z. Ionic gels and their applications in stretchable electronics. *Macromol. Rapid Commun.* **2018**, *39*, 1800246.

[124] Tang, S.; Sha, D.; He, Z.; Chen, X.; Ma, Y.; Liu, C.; Yuan, Y. Environmentally adaptable organo-ionic gel-based electrodes for real-time on-skin electrocardiography monitoring. *Adv. Healthcare Mater.* **2023**, *12*, 2300475.

[125] Song, S.; Choi, H.-S.; Cho, C.-H.; Lim, S. K.; Jeong, S. M. Bright and uniform light emission from stretchable, dual-channel energy conversion systems: simultaneous harnessing of electrical and mechanical excitations. *Appl. Phys. Rev.* **2022**, *9*, 011423.

[126] Sun, J.; Chang, Y.; Liao, J.; Chang, S.; Dai, S.; Shang, Y.; Shan, C.-X.; Dong, L. Integrated, self-powered, and omni-transparent flexible electroluminescent display system. *Nano Energy* **2022**, *99*, 107392.

[127] Yoo, J.; Li, S.; Kim, D.-H.; Yang, J.; Choi, M. K. Materials and design strategies for stretchable electroluminescent devices. *Nanoscale Horiz.* **2022**, *7*, 801–821.

[128] Yu, S.; Park, T. H.; Jiang, W.; Lee, S. W.; Kim, E. H.; Lee, S.; Park, J.-E.; Park, C. Soft human-machine interface sensing displays: materials and devices. *Adv. Mater.* **2023**, *35*, 2204964.

[129] Oh, S.-J.; Choi, S.-E.; Woo, I.; Yoon, J. U.; Bae, J.; Bae, J. W. Stretchable multicolored electroluminescent sound display for wearable and interactive textiles. *Adv. Funct. Mater.* **2025**, *35*, 2420432.

[130] Lin, Y.; Chen, W.; Ye, J.; Xu, J.; Gan, X.; Peng, Y.; Zhou, X.; Guo, T.; Zhang, Y.; Wu, C. Ingenious integration of electroluminescent devices with natural triboelectrification for wearable display by using epidermal potential as stimulation bridge. *Opt. Mater.* **2023**, *137*, 113627.

[131] Wang, X.; Lin, Y.; Zhang, Y.; Xu, S.; Liu, M.; Shen, Y.; Gong, Y.; Xiong, Y.; Hu, Y. Coplanar pattern and temperature transient control in intelligent

wearable multi-color alternating current electroluminescence devices. *Adv. Funct. Mater.* **2025**, *35*, 2420613.

[132] Yang, D.; Zhao, Y.; Du, X.; Lu, Y.; Zhang, X.; Qin, J.; Yin, Y.; Zhong, Z.; Wang, D.; Yang, Z. et al. Multi-stimulus responsive multicolor electroluminescent PDLCs for multimodal anti-counterfeiting and wide color gamut display. *Adv. Funct. Mater.* **2025**.

[133] Zhou, Z.; Zheng, Y.; Zhang, Y.; Lu, Y.; Liu, P.; Wu, J.; Wang, B.; Qin, J.; Peng, H.; Chen, P. Large-area writable textile display via parallel-aligned electroluminescent fibers and field-activated dielectric inks. *Adv. Funct. Mater.* **2025**.

[134] Cho, S.; Chang, T.; Yu, T.; Gong, S. Machine embroidery of light-emitting textiles with multicolor electroluminescent threads. *Sci. Adv.* **2024**, *10*, eadk4295.

[135] Shin, Y. B.; Ju, Y. H.; Lee, H.-J.; Han, C. J.; Lee, C.-R.; Kim, Y.; Kim, J.-W. Self-integratable, healable, and stretchable electroluminescent device fabricated via dynamic urea bonds equipped in polyurethane. *ACS Appl. Mater. Interfaces* **2020**, *12*, 10949–10958.

[136] Zhang, X.; Ye, T.; Meng, X.; Tian, Z.; Pang, L.; Han, Y.; Li, H.; Lu, G.; Xiu, F.; Yu, H.-D. et al. Sustainable and transparent fish gelatin films for flexible electroluminescent devices. *ACS Nano* **2020**, *14*, 3876–3884.

[137] Chen, L.; Wong, M.-C.; Bai, G.; Jie, W.; Hao, J. White and green light emissions of flexible polymer composites under electric field and multiple strains. *Nano Energy* **2015**, *14*, 372–381.

[138] Zhang, J.; Lu, Q.; Wu, M.; Sun, Y.; Wang, S.; Wang, X.; Lu, M.-H.; Kong, D. Intrinsically stretchable light-emitting drawing displays. *npj Flexible Electron.* **2024**, *8*. 1.

[139] Oh, S.; Lee, S.; Byun, S. H.; Lee, S.; Kim, C. Y.; Yea, J.; Chung, S.; Li, S.; Jang, K. I.; Kang, J. et al. 3D shape-morphing display enabled by electrothermally responsive, stiffness-tunable liquid metal platform with

stretchable electroluminescent device. *Adv. Funct. Mater.* **2023**, *33*, 2370149.

[140] Guo, J.; Guo, F.; Zhao, H.; Yang, H.; Du, X.; Fan, F.; Liu, W.; Zhang, Y.; Tu, D.; Hao, J. In-sensor computing with visual-tactile perception enabled by mechano-optical artificial synapse. *Adv. Mater.* **2025**, *37*.

[141] Liu, Y.; Wang, T.; Sun, Z.; Liu, C.; Han, L.; Liu, R.; Liu, Y.; Zhou, Y. Nature-inspired pressure interactive alternating current electroluminescent for orientation indication, visual sensing, and remote monitoring. *Adv. Mater. Technol.* **2023**, *8*, 2301289.

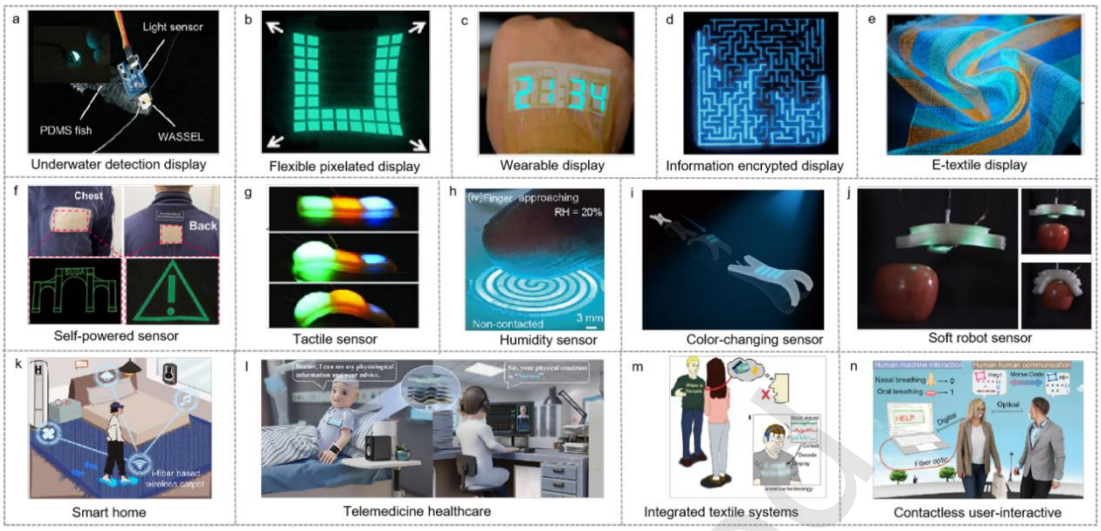

Figure 1. Applications of ACEL devices include (a) underwater detection display (Reproduced with permission from Ref. [35] Copyright 2024, Wiley-VCH), (b) flexible pixelated display (Reproduced with permission from Ref. [36] Copyright 2019, American Chemical Society), (c) wearable display (Reproduced with permission from Ref. [37] Copyright 2019, American Chemical Society), (d)information encrypted display (Reproduced with permission from Ref. [38] Copyright 2024, Wiley-VCH), (e) e-textile display (Reproduced with permission from Ref. [39] Copyright 2021, Springer Nature), (f) self-powered sensor (Reproduced with permission from Ref. [40] Copyright 2022, Elsevier Ltd), (g) tactile sensor (Reproduced with permission from Ref. [41] Copyright 2016, The American Association for the Advancement of Science), (h) humidity sensor (Reproduced with permission from Ref. [42] Copyright 2024, Wiley-VCH), (i) color-changing sensor (Reproduced with permission from Ref. [43] Copyright 2022, Springer Nature), (j) soft robot sensor (Reproduced with permission from Ref. [44] Copyright 2019, Springer Nature), (k) smart home (Reproduced with permission from Ref. [45] Copyright 2024, The American Association for the Advancement of Science), (l)telemedicine healthcare (Reproduced with permission from Ref. [46] Copyright 2024, Wiley-VCH), (m) integrated textile systems (Reproduced with permission from Ref. [39] Copyright 2021, Springer Nature), (n) contactless user-interactive (Reproduced with permission from Ref. [42] Copyright 2024, Wiley-VCH).

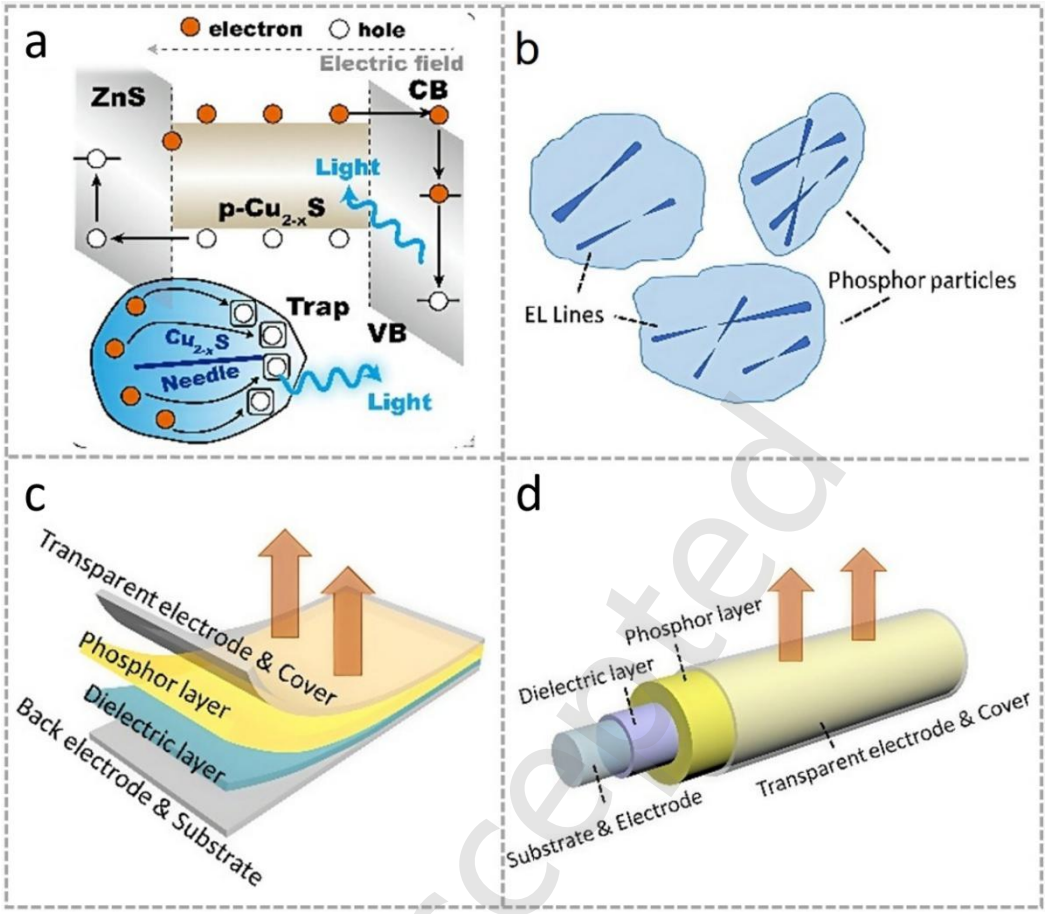

Figure 2. Mechanisms of different types of ACEL devices. (a) Light emitting mechanism of flexible ACEL devices (Reproduced with permission from Ref. [49] Copyright 2025, Royal Society of Chemistry). (b) Schematic diagram of EL lines inside the phosphor particles (Reproduced with permission from Ref. [40] Copyright 2021, American Chemical Society). (c) Structure diagram of a Planar flexible ACEL device (Reproduced with permission from Ref. [40] Copyright 2021, American Chemical Society). (d) Structure diagram of a fiber-like flexible ACEL device (Reproduced with permission from Ref. [40] Copyright 2021, American Chemical Society).

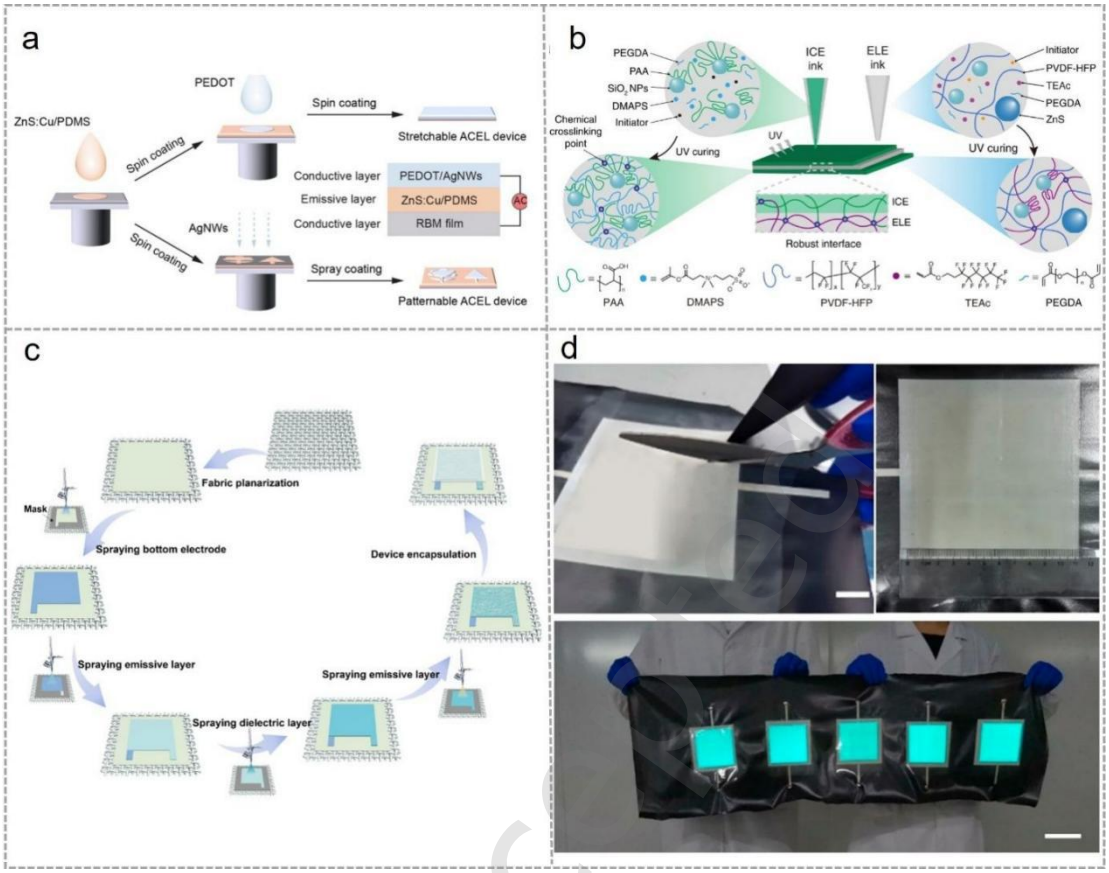

Figure 3. Schematic diagrams of four typical processes for preparing flexible ACEL devices. (a) Spin coating: A uniform thin film is formed over a large area by depositing the slurry onto a substrate, which is then spun at high speed to spread the material by centrifugal force (Reproduced with permission from Ref. [62] Copyright 2025, The American Association for the Advancement of Science). (b) Printing: High-precision, non-contact patterned deposition of inks is achieved through digital control (Reproduced with permission from Ref. [43] Copyright 2022, Springer Nature). (c) Spray coating: An aerosolized slurry is deposited onto the substrate using a spray gun, suitable for complex curves and large-area rapid coating (Reproduced with permission from Ref. [63] Copyright 2024, American Chemical Society). (d) Screen printing: The slurry is transferred through a patterned mesh screen onto the substrate, suitable for preparing functional patterns of high thickness (Reproduced with permission from Ref. [64] Copyright 2021, American Chemical Society).

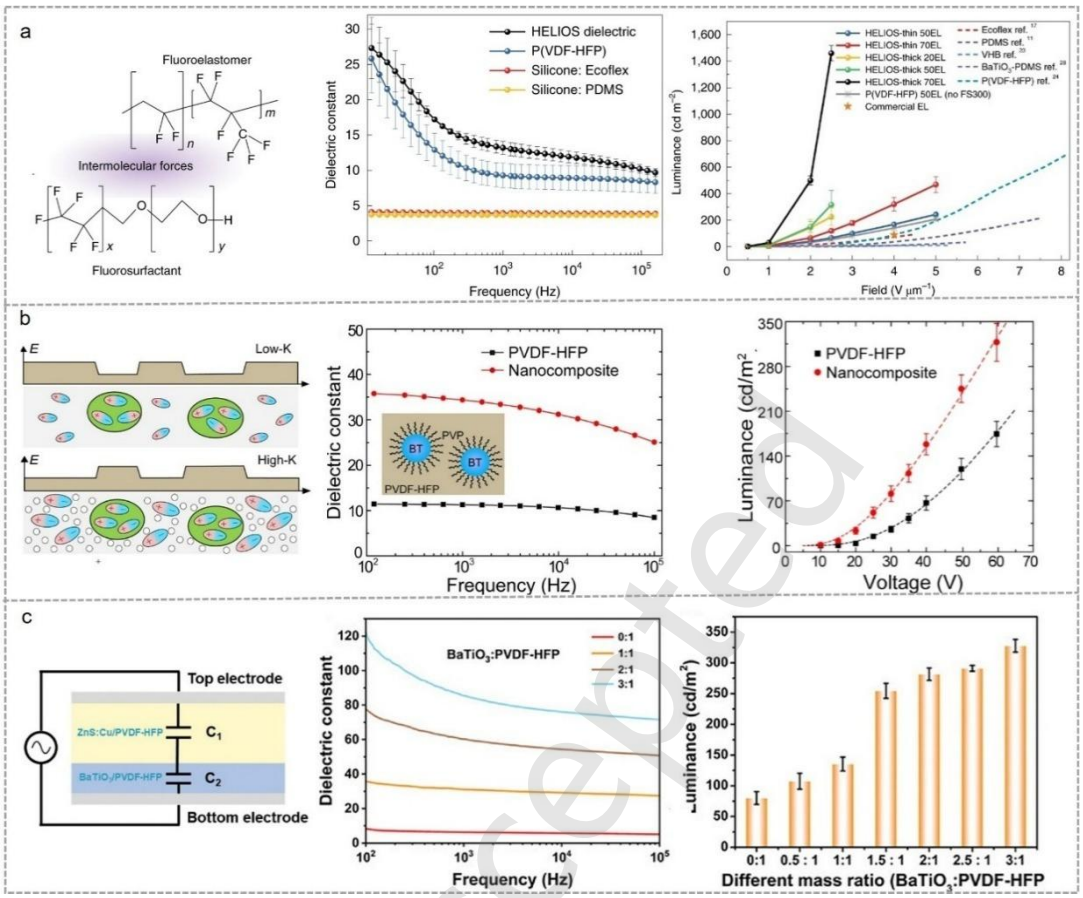

Figure 4. Application of dielectric materials with distribution and properties in flexible ACEL devices. Frequency-dependent dielectric constants and the luminescence of ACEL devices based on these dielectric materials under different voltages regarding (a) device without independent dielectric layer (Reproduced with permission from Ref. [44] Copyright 2019, Springer Nature); (b) composite structure with dielectric filler/luminescent powder blend (Reproduced with permission from Ref. [37] Copyright 2019, American Chemical Society); (c) a layered structure with a separate dielectric layer (Reproduced with permission from Ref. [80] Copyright 2023, Wiley-VCH).

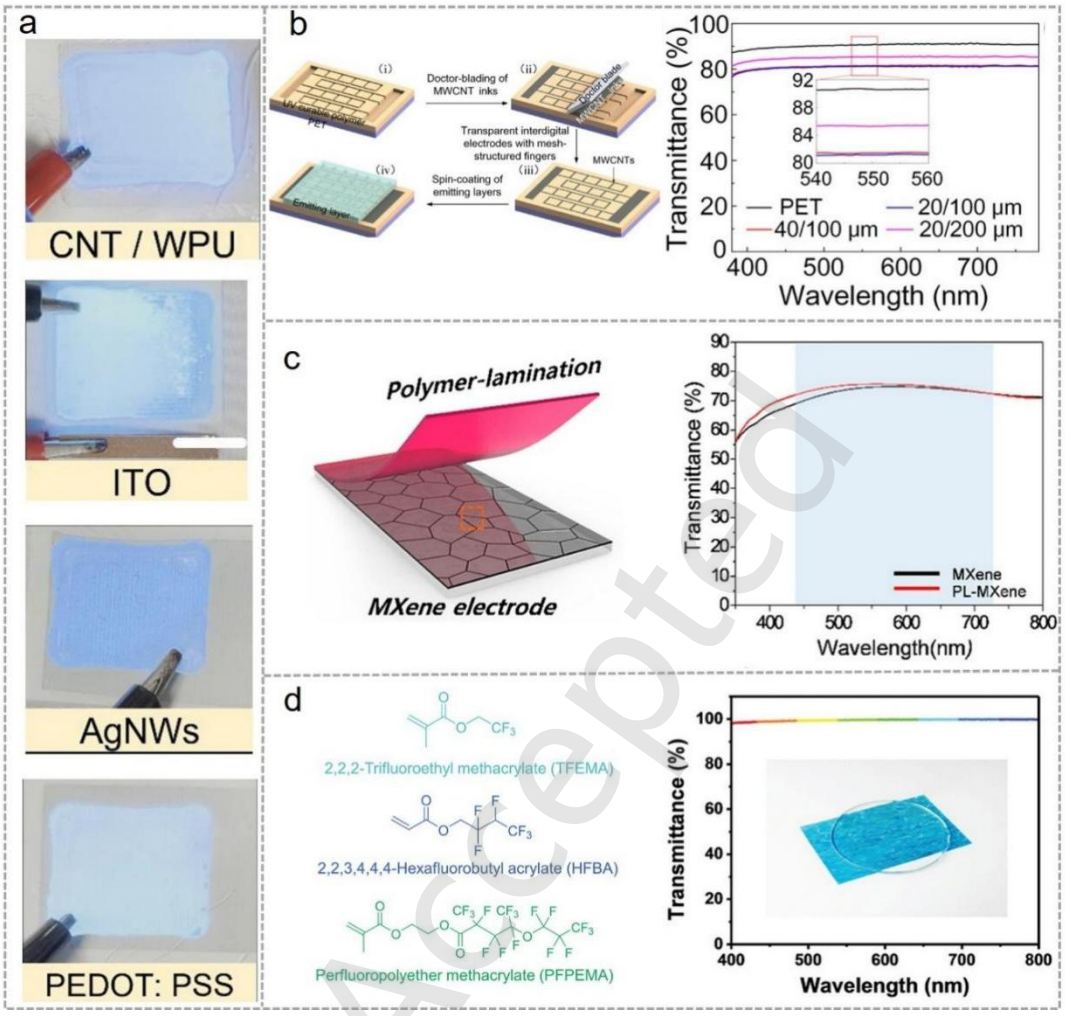

Figure 5. Performance comparison of various transparent electrodes in flexible ACEL devices. (a) Digital images of four typical transparent electrode materials (CNT/WPU, ITO, AgNWs, PEDOT:PSS) (Reproduced with permission from Ref. [63] Copyright 2024, American Chemical Society). (b)Transmittance curve of MWCNTs electrodes (Reproduced with permission from Ref. [109] Copyright 2020, American Chemical Society). (c) Micromorphology and transmittance of MXene electrodes (Reproduced with permission from Ref. [110] Copyright 2021, American Chemical Society). (d) Physical image and transparency curve of ionic gel electrodes (Reproduced with permission from Ref. [35] Copyright 2024, Wiley-VCH).

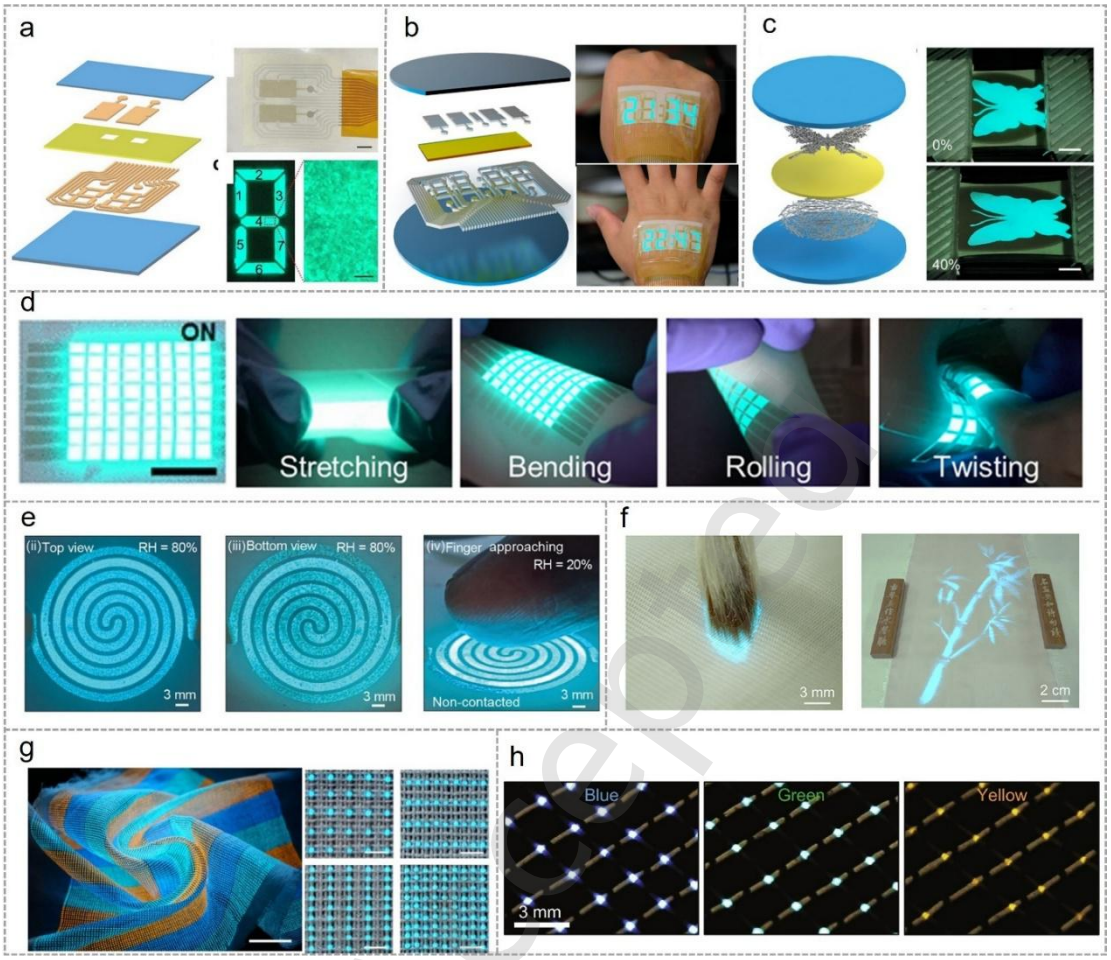

Figure 6. Patterned display based on flexible ACEL devices. (a) Schematic of a simple digital display (Reproduced with permission from Ref. [74] Copyright 2024, American Chemical Society). (b) Schematic of a four-digit seven-segment display (Reproduced with permission from Ref. [37] Copyright 2019, American Chemical Society). (c) Schematic of a butterfly display (Reproduced with permission from Ref. [90] Copyright 2018, American Chemical Society). (d) Schematic of an 8×8 pixel ACEL device and photographs of ACEL device illumination under stretching, bending, rolling, and twisting (Reproduced with permission from Ref. [36] Copyright 2019, American Chemical Society). (e) Top and bottom views of the ACEL under 80% relative humidity after power on, and photographs of luminescence response under 20% relative humidity (Reproduced with permission from Ref. [42] Copyright 2024, Wiley-VCH). (f) Detail photographs of brush-written text on the display fabric and a drawn bamboo pattern (Reproduced with permission from Ref. [133] Copyright 2025, Wiley-VCH). (g) Digital images of fabric display units with varying distances

achieved by changing weaving parameters (Reproduced with permission from Ref. [39] Copyright 2021, Springer Nature). (h) Digital images of fabric display units in different colors (Reproduced with permission from Ref. [134] Copyright 2023, The American Association for the Advancement of Science).

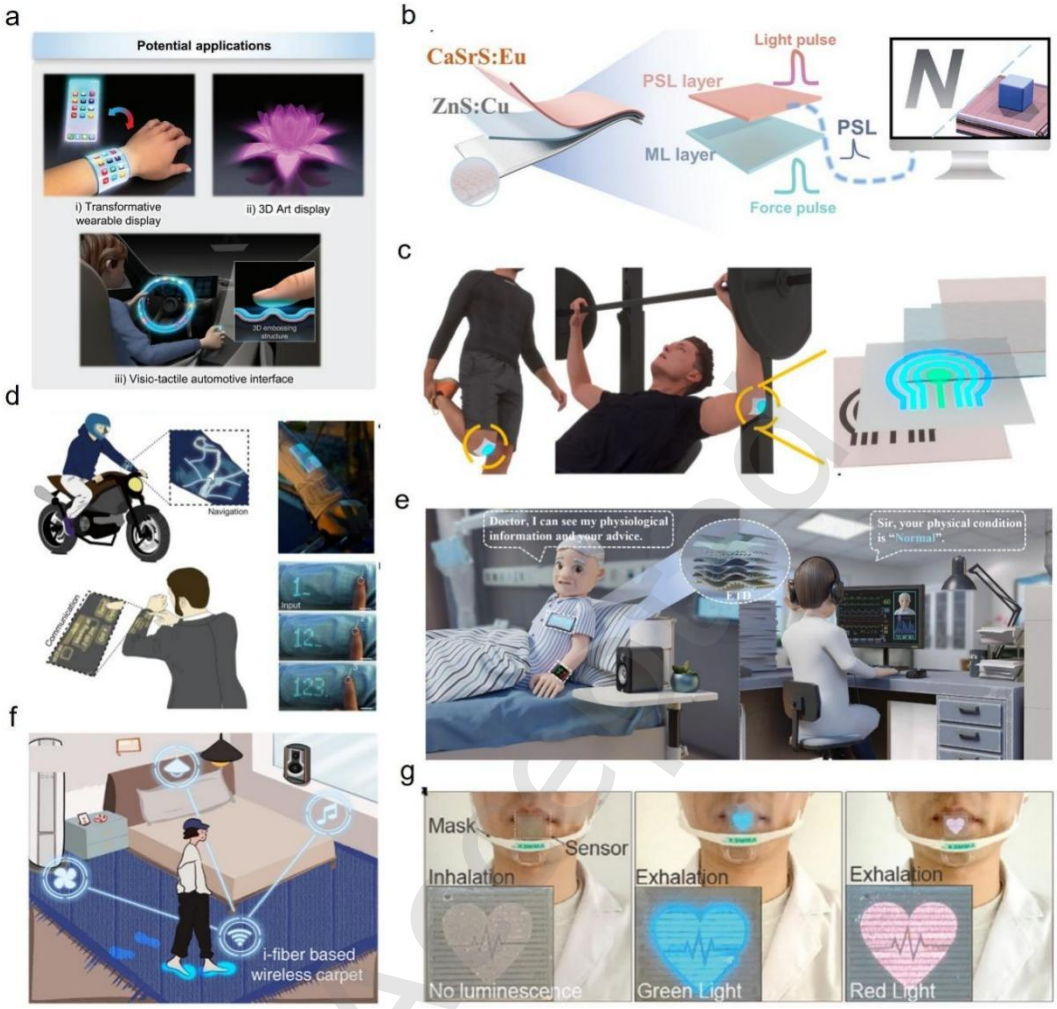

Figure 7. Emerging applications of flexible ACEL devices in interactive displays, showcasing their role in human-machine interaction, health monitoring, and the IoT. (a) By integrating display functions with sensing and communication technologies, various innovative solutions are realized, including a visual-haptic feedback system (Reproduced with permission from Ref. [139] Copyright 2023, Wiley-VCH) (b) joint activity monitoring (Reproduced with permission from Ref. [140] Copyright 2024, Wiley-VCH) (c) intelligent textile nodes (Reproduced with permission from Ref. [63] Copyright 2024, American Chemical Society) (d) telemedicine (Reproduced with permission from Ref. [39] Copyright 2021, Springer Nature) (e) wireless appliance control (Reproduced with permission from Ref. [46] Copyright 2024, Wiley-VCH) (f) and interactive breathing masks (Reproduced with permission from Ref. [45] Copyright 2024, The American Association for the Advancement of Science) (g) revealing their immense potential in achieving intelligent integration of

"human-machine-object" (Reproduced with permission from Ref. [42] Copyright 2024, Wiley-VCH).